nature reviews chemistry

https://doi.org/10.1038/s41570-023-00534-6

Review article

Check for updates

Strategic application of C–H oxidation in natural product total synthesis

Ian Bakanas[1,2], Robert F. Lusi[1,2], Stefan Wiesler[1], Jack Hayward Cooke[1] & Richmond Sarpong[1]

Abstract

The oxidation of unactivated C–H bonds has emerged as an effective tactic in natural product synthesis and has altered how chemists approach the synthesis of complex molecules. The use of C–H oxidation methods has simplified the process of synthesis planning by expanding the choice of starting materials, limiting functional group interconversion and protecting group manipulations, and enabling late-stage diversification. In this Review, we propose classifications for C–H oxidations on the basis of their strategic purpose: type 1, which installs functionality that is used to establish the carbon skeleton of the target; type 2, which is used to construct a heterocyclic ring; and type 3, which installs peripheral functional groups. The reactions are further divided based on whether they are directed or undirected. For each classification, examples from recent literature are analysed. Finally, we provide two case studies of syntheses from our laboratory that were streamlined by the judicious use of C–H oxidation reactions.

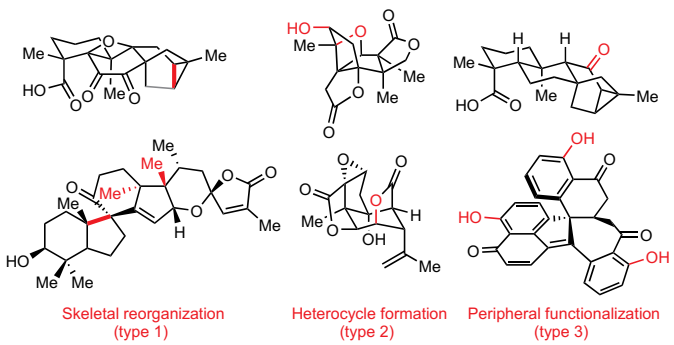

Sections

[1]Department of Chemistry, University of California, Berkeley, Berkeley, CA, USA. [2]These authors contributed equally: Ian Bakanas, Robert F. Lusi. e-mail: rsarpong@berkeley.edu

Key points

- C–H oxidation reactions of unactivated bonds have found increased application as key enabling steps in complex molecule synthesis.
- Strategically, C–H oxidation reactions can serve the purpose of making, breaking or rearranging skeletal bonds (type 1), forming heterocyclic rings (type 2), and introducing peripheral functional groups (type 3).
- From the many C–H bonds in a molecule, site-selectivity for oxidations can be guided by substrate sterics and electronics and/or supramolecular control (undirected) or by inherent functional groups (directed).
- C–H oxidation reactions enable conversion of structurally complex, but readily available, starting materials to useful intermediates through introduction of remote functionalization.
- Remote functionalization can be further leveraged to generate target-oriented complexity, that is, elimination, rearrangement, C–C bond formation and so on.
- The logic of C–H oxidation reactions can be combined with traditional synthetic planning strategies to devise highly efficient and divergent syntheses.

Introduction

Available reaction methodologies dictate synthesis planning. The development of new methods enables new strategies that might have been previously considered unfeasible. Methodologies that oxidize unactivated C–H bonds allow one to reimagine what is possible in synthesis because they enable the conversion of ubiquitous, and typically inert, C–H bonds to versatile functional handles[1–4]. The central challenge of applying C–H oxidation in complex molecule synthesis lies in distinguishing a targeted C–H bond from the many other C–H bonds in a molecule. To address this challenge, C–H oxidation methodologies with distinct and complementary selectivity rules have been developed rapidly[5–13]. Total synthesis is the ultimate testing ground for methodology and, as such, C–H oxidation-based strategies for the synthesis of complex natural products have gained in popularity in recent years[14–22]. Although the application of these reactions in synthesis has been the topic of several reviews[15,18,21,22], our understanding of them and the strategies they enable continues to evolve. A thorough understanding of the rules that govern selectivity in C–H oxidation and the way the outcome of such reactions might be affected in a complex molecular context is important for their broad adoption. This reality is also reflected in the fact that far more methods have been discovered than have been applied in total synthesis[23–25]. Nevertheless, strategies for total synthesis reliant on C–H oxidation have emerged, such as the 'two-phase' synthesis approach codified by Baran[26–29], in which the cores of molecules are constructed rapidly in the 'cyclase phase' followed by peripheral functionalization in the 'oxidase phase' and feedstock-based oxidative approaches[30], in which oxidation is used to remodel the carbon skeleton of an abundant starting material. In our own laboratory, C–H oxidation reactions have been crucial to the success of numerous total syntheses[31–41]. Additional strategies tend to emerge as synthetic chemists continue to demonstrate that these methods have the potential to streamline synthesis routes or make a single route applicable to a wider variety of targets.

Our analysis indicates that C–H oxidation reactions in complex molecule synthesis generally fall into one of three types on the basis of their strategic purpose (Fig. 1). Although these C–H oxidation types are subjective, and there are exceptions that do not align with our categorization, we contend that they provide a useful framework for considering how these reactions might enable a strategy to construct a target molecule. All types of C–H oxidation reactions may introduce a variety of functional groups in the immediate product, but for the classifications presented in this Review, we only consider the ultimate purpose of the reaction in the context of the target molecule. Our definitions of the types of C–H oxidation are as follows:

- Type 1: installs functionality that is used, either transiently or over the course of subsequent steps, to establish the carbon skeleton of the target molecule
- Type 2: constructs a heterocyclic ring that appears in the target molecule
- Type 3: installs one or more of the peripheral functional groups of the target molecules

Overall, these classifications focus on how oxidation is used to construct structural elements of the target molecule without considering intermediates en route to this goal. For example, the use of C–H oxidation to install a hydroxy group that is then used to initiate a cationic rearrangement to the skeleton of the target molecule would be classified as a type 1 oxidation despite initially proceeding through a hydroxy group. Likewise, a desaturation reaction could convert C–H bonds to a double bond that could undergo further dihydroxylation to install peripheral hydroxy groups in a process that is a type 3 use of oxidation. These categories may be further subdivided by whether the C–H oxidation reaction proceeds in a 'directed'[42–46] or 'undirected'[47] manner, affording six possible strategic scenarios for a C–H oxidation reaction. We will highlight examples of each classification in syntheses published after 2020, in which the usage of C–H oxidation enabled uniquely efficient synthesis planning. Finally, we will provide insight into the thought processes and synthesis planning that guided syntheses from our own laboratory that utilize several different C–H oxidations. Brief primers on the fundamentals of undirected and directed functionalizations are provided in Boxes 1 and 2. As this review will mostly focus on the application of C–H oxidation in complex molecule synthesis, the reader is encouraged to consult reviews on C–H oxidation methodology for an in-depth analysis[10–12,14,15,17,20].

Type 1 C–H oxidation

Type 1 C–H oxidations, as defined here, facilitate the construction, cleavage or rearrangement of skeletal C–C bonds. As such, they have been more frequently deployed early in syntheses and have found particular application in bioinspired syntheses, in which the newly introduced oxidation allows access to carbocationic intermediates that undergo transformations analogous to those in the biosynthesis of a molecule. A practical advantage of using C–H oxidation approaches is that an expanded set of readily available natural products (for example, the 'chiral pool')[48,49] can be considered strategic starting materials, despite being distantly related to or lacking the requisite oxidation of the target. In the next two sections we discuss several examples in which advanced starting materials — steroids and diterpenes — are transformed by introducing unnatural oxidation so that minimal synthetic effort is expended on elaborating the carbon skeleton.

Undirected Type 1 C–H oxidation

In their synthesis of complex diterpenes (Fig. 2), Renata and colleagues leverage enzymatic and chemical methods to selectively oxidize 11 different positions in four distinct terpene scaffolds[50], accessing eight diterpenoids in rapid fashion from abundant, lower oxidation-state, terpenoid feedstocks (Fig. 2a). Although we will only discuss their synthesis of mitrephorone A, the site and type of each oxidation used in their collective terpene syntheses are highlighted in Fig. 2a. Recognition of the biosynthetic relationships between the targeted diterpenoid families was key to their approach. For example, the [3.2.1] bicycle of the *ent*-beyerane family and the [2.2.2] bicycle of the *ent*-atisane family are related through a Wagner–Meerwein shift (Fig. 2b, **1** to **2**), and the *ent*-trachylobane family, bearing a [3.2.1.0] tricycle, can arise from a cationic cyclization of the *ent*-atisane scaffold (**3** to **4**), and vice versa[51]. Starting from the cheap, abundant *ent*-beyerane isosteviol (**5**), a series of bioinspired rearrangements enabled conversion to the *ent*-atisane skeleton and, subsequently, the complex *ent*-trachylobane mitrephorone A[52] (**11**). This strategy depended on the development of a biocatalytic, site-selective C-12 oxidation of isosteviol (**5**), which could be leveraged to form the required carbocation.

Biocatalysis is a promising modality for achieving undirected C–H oxidations. The specific and tunable arrangement of the active site of an enzyme allows the positioning of substrates for site-selective oxidation by a reactive cofactor (often an iron haem) under mild reaction conditions. Thus, such reactions could theoretically be applied to target any position on any molecule[53–59]. Several enzymes were identified from the platensimycin biosynthesis, PtmO5, PtmO3 and PtmO6, which promiscuously accept *ent*-kaurane substrates[60,61]. Among these enzymes, the P450 monooxygenase (PtmO5) was found to be effective for oxidation of the *ent*-beyerane isosteviol (**5**) that serendipitously underwent selective C-12 oxidation. Renata et al. hypothesize that the observed selectivity arises from the different binding positions of the *ent*-kaurane and *ent*-beyerane skeletons within the active site. Using PtmO6 and PtmO5, site-selective and chemo-selective oxidization of four different positions on different diterpene feedstocks was achieved.

In their synthesis of mitrephorone A (Fig. 2c, **11**), Renata and colleagues began from isosteviol (**5**), which underwent a selective, undirected type 1 C–H oxidation to alcohol **6** on preparative scale, using a PtmO5 chimera protein. The envisaged skeletal reorganization was then initiated through the ionization of **6** with TfOH to form *ent*-beyeryl cation **7**, followed by a 1,2-acyl shift and elimination to afford the *ent*-atisane skeleton. The reduction of the ketone group with L-selectride® gave alcohol **8**, which was primed to undergo the second of the two skeletal rearrangements. $BF_3{\cdot}OEt_2$-mediated ionization and selective reduction of the resulting non-classical carbocation (**9**) by triethylsilane gave *ent*-trachylobane acid **10** in 61% yield over three cycles, which was elaborated to mitrephorone A (**11**) in just five additional steps—a total nine steps.

It is important to highlight how the development of new C–H oxidation methodologies enabled a highly concise synthesis of mitrephorone A (**11**; previous syntheses: 18 and 23 steps)[62,63] by making isosteviol (**5**), which has the same number of carbon atoms as the target molecule, a viable starting material. The subsequent skeletal reorganizations were only possible as a result of the selective remote C–H oxidation of the C-12 position, achieved through an undirected C–H oxidation. In turn, these key transformations relied on a detailed knowledge of terpene biosynthesis, both in terms of the carbocationic rearrangements and identifying the specific oxidation enzymes.

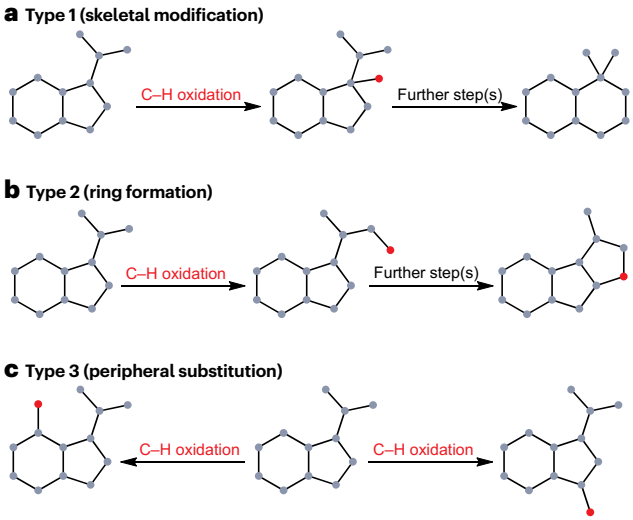

Fig. 1 | Strategic use and cases of C–H oxidation. a, Type 1 C–H oxidation reactions aim to modify the carbon skeleton of the target molecule. **b**, Type 2 C–H oxidation reactions allow for the construction of a heterocyclic ring in the target molecule. **c**, Type 3 C–H oxidation reactions focus on installation of one or more functional groups on the target molecule.

Directed type 1 C–H oxidation

In 2022, Heretsch et al.[64] and Deng et al.[65] published contemporaneously on the synthesis of spirochensilide A[66] (**15**) from lanosterol (**16**) using similar bioinspired strategies (Fig. 3). On the basis of analyses of known congeners of lanosterol (**16**), both groups proposed an updated biosynthetic pathway (Fig. 3a). They hypothesized that lanosterol undergoes several enzymatic oxidations to afford diepoxide **12**, which is followed by selective ring opening of the northern epoxide to give carbocation **13**. Two successive Wagner–Meerwein shifts would set the distinctive methyl group pattern, and the remaining epoxide (**14**) would then undergo a Meinwald rearrangement to install the eponymous spirocycle found within the core of spirochensilide A (**15**). By targeting intermediates analogous to carbocation **13**, lanosterol could be used as an advanced starting material bearing all the requisite carbons. However, site-selective undirected C–H oxidation at C-17 appeared challenging given the multiple tertiary electron-rich C–H bonds and double bonds of lanosterol. Both groups opted to use directed C–H oxidations.

The synthesis of Heretsch et al.[64] (Fig. 3b) commenced by cleaving the alkene of the prenyl side-chain of lanosterol (**16**), leveraging this latent functionality to install a hydroxy group subsequently used to direct the required C–H oxidation. Upon treating alcohol **17** with modified Suárez reaction conditions (NaI, phenyliodine diacetate (PIDA) and visible-light irradiation)[67], the formation of an alkoxy radical was followed by selectivity-determining 1,5-HAT of the C-17 H-atom. The resulting tertiary radical was then further oxidized to carbocation **18**, probably via the corresponding alkyl iodide, which triggered the first of the two bioinspired Wagner–Meerwein shifts; trapping by the pendent hydroxy group gave rearranged tetrahydropyran product **19** in 34% yield. The second shift was initiated by the ionization of the ring with $TiCl_4$, and the subsequent elimination afforded diene **20** in excellent yield. The final phase of their skeletal reorganization was achieved by oxidative rearrangement of **20** by treatment with *N*-iodosuccinimide and $AgNO_3$ in a hexafluoroisopropanol:water mixture. The authors

Box 1

Undirected C–H oxidation fundamentals

Site-selectivity rules for electrophilic C–H oxidation

- Oxidations that proceed through different mechanisms can have different selectivity rules
- Site-selectivity is based on substrate electronics and steric accessibility
- These factors can be tuned by oxidant choice and the introduction of electron-withdrawing or electron-releasing groups to perturb electronics

Examples using common TFDO or White–Chen (WC) catalyst

- Not compatible with nucleophilic functional groups (alkenes, amines, alcohols and so on)
- Most successfully applied in targeting electron-rich methynes or methylenes when using sterically bulky catalysts

Supramolecular control

- Supramolecular encapsulation can override substrate control through positioning of the substrate in active site
- Biocatalytic C–H oxidations have been particularly effective for evolvable site-selectivity
- Figure reprinted with permission from ref. 59, ACS

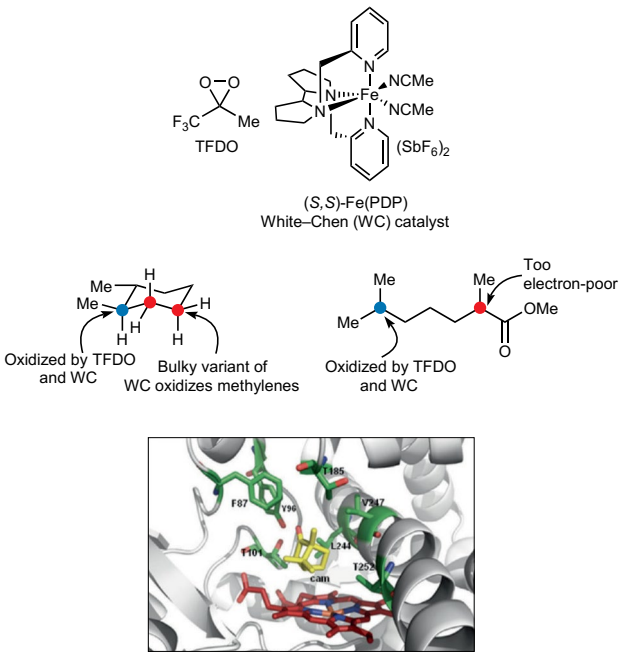

proposed that epoxidation of the tetra-substituted alkene group proceeds via the corresponding halohydrin, and a subsequent bioinspired Meinwald rearrangement affords spirocycle **21**. The synthesis was completed in an additional eight steps, a sequence that is notably shorter than the previous 22-step synthesis[68], once again owing to the advanced starting position.

The synthesis of Deng and co-workers[65] (Fig. 3c) relied on a similarly effective recognition of lanosterol as a starting material. However, instead of triggering the rearrangements in a stepwise fashion, they endeavoured to do so in a single operation. From lanosterol (**16**), the two-step cleavage of the tri-substituted alkene unveiled aldehyde **22**, which was homologated to trifluoromethyl ketone **23** by addition of $TMSCF_3$ and the subsequent oxidation by Dess–Martin periodinane (DMP). Treating trifluoromethyl ketone **23** with oxone formed the corresponding dioxirane, which subsequently underwent intramolecular C–H insertion at the proximal and weak C-17 C–H bond to give the trifluoromethyl hemiketal, which was saponified and methylated to give alcohol **24** in 50% yield over two steps. Yang et al. have previously leveraged trifluoromethyl ketones for intramolecular C–H oxidation[69–72], although the report of Deng and colleagues, to our knowledge, may be the first such application in total synthesis. Three additional steps afforded bisepoxide **25**, setting the stage for the rearrangement cascade. The treatment of bisepoxide **25** with an excess of $BF_3{\cdot}OEt_2$ triggered all three of the bioinspired rearrangements to give spirocycle **26** in 35% yield that was elaborated to spirochensilide A in seven steps.

Together, these syntheses clearly highlight the power of C–H oxidation as an entry point into carbocationic rearrangements, exemplifying how oxidation can be leveraged to reshape a carbon skeleton and build target-oriented complexity in a type 1 manner. Whereas type 1 C–H oxidation-based strategies have most commonly found application in enabling rearrangements, one could also envision using these reactions for C–C bond formation or cleavage. For example, a terpene could be functionalized using C–H oxidation, and the resulting functional handle could be used to synthesize sesquiterpenes or diterpenes through prenylation. Alternatively, one could envision taking a readily available, more structurally complex starting material—higher-order terpenoids, steroids and so on—that contains a target relevant sub-skeleton and using C–H oxidation to install a functional handle to mediate C–C cleavage reactions to yield a less structurally complex but more synthetically valuable intermediate. Continued development of C–H oxidation methodologies will, therefore, allow for new simplifying strategies to become viable approaches in synthesis planning, particularly by expanding the complexity of the feedstocks that can be considered as strategic starting points.

Type 2 C–H oxidation

We define type 2 C–H oxidations as those that result in the formation of heterocyclic rings of a target molecule. Ether and lactone linkages are prevalent structural elements in many natural products, such as highly oxidized terpenes[73,74]. Type 2 C–H oxidation has, therefore, found great use in total synthesis; however, this has primarily been in the form of directed Suárez oxidations[75] or carboxylate-directed lactonizations mediated by the White–Chen catalyst[76]. Undirected type 2 oxidation strategies are somewhat underexplored but can be especially effective in divergent syntheses to access multiple natural products that bear different heterocyclic ring patterns.

Undirected type 2 C–H oxidation

In a recent synthesis of Zhang and colleagues (Fig. 4), an incisive late-stage desaturation was used in order to access several high-oxidation state *Illicium* sesquiterpenes[77–79]. The versatility of the introduced unsaturation is evident in its use as a handle for epoxidation, hydration and allylic oxidation—all of which are used to make natural

Box 2

Directed C–H oxidation fundamentals

Innate oxidation

- Relies on inherently reactive functional groups
- Site-selectivity is governed by innate geometry
- For hydrogen atom transfer (HAT)-based mechanisms, 1,5-HAT is preferred and most common

Tethered oxidation

- Utilizes a tethered group (TG) often appended to a heteroatom
- TG either acts as directing group or reacts directly with desired C–H bond
- Site-selectivity is variable on the basis of the tether choice and length

Directed metalation

- Utilizes a directing group (DG) to guide a metal to the desired C–H bond
- Lowers kinetic barrier to activation
- Site-selectivity is governed by the size of metallocycle, often five-membered

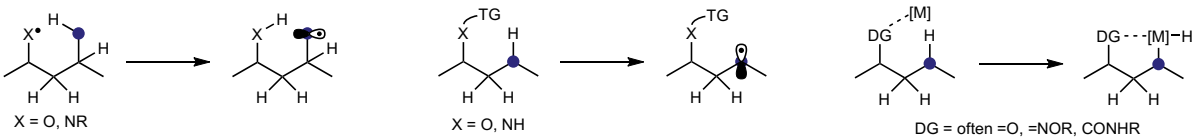

products. This synthesis highlights an underused synthetic strategy in which electron-rich C–H bonds can be targeted as latent alkenes through halogenation then elimination, hydroxylation–elimination or direct desaturation.

The Zhang synthesis commenced from *R*-pulegone (**33**) (Fig. 4b), which underwent a Favorskii ring contraction and subsequent allylation to give ester **34** in 85% yield as a single diastereomer over two steps. Crucially, the unactivated tertiary stereocenter of *R*-pulegone imparts diastereoselectivity in the allylation reaction but is ultimately ablated in the linchpin type 2 desaturation reaction later in the synthesis. This elegant strategy once again demonstrates how C–H oxidation can enable the unconventional use of chiral-pool feedstocks, as the stereocenter of *R*-pulegone serves to provide enantiospecific entry to the *Illicium* sesquiterpenes, controls the installation of additional elements of stereochemistry and is leveraged as a latent alkene functional handle for late-stage diversification to the natural product family. With **34** in hand, epoxidation of the tetra-substituted alkene group with *meta*-chloroperbenzoic acid and oxidative cleavage of the allyl group with $RuCl_3$ and $NaIO_4$ proceeded with spontaneous lactonization to give bicycle **35** in 77% yield. Following a sequence of four steps, propargylic alcohol **36** was prepared and subjected to palladium-catalysed borylative-cyclization[80,81] conditions that yielded alcohol **37** after an oxidative work-up. In two additional steps, selenocarbonate **38** was prepared and a radical cyclization initiated by azobisisobutyronitrile was performed to close the last core ring to give **27** in 96% yield. The key desaturation was then investigated. Calculated bond dissociation energies (BDEs) predicted that the C-7 α-hydroxy bond was weaker than the desired C–H bond by 3.2 kcal mol^{-1}. To overcome this undesired selectivity, Zhang et al. hypothesized that tuning the electronic and steric environment of the secondary alcohol through hydrogen bonding could affect the BDE and rate of oxidation at C-7[82]. Using hexafluoroisopropanol as solvent, with 390 nm violet LED initiation and benzophenone as a triplet sensitizer, undesired reactivity at C-7 was suppressed, giving alkene **28** in 82% yield on gram-scale.

This oxidation was relayed in a type 2 fashion to synthesize merrilactone A[83] (**29**) and anislactone B[84] (**30**) (Fig. 4c). First, alkene **28** was epoxidized and then treated with *para*-toluenesulfonic acid to induce ether bridge formation — installing the heterocycle characteristic of a type 2 oxidation — completing the synthesis of merrilactone A in 13 steps[85,86] in a remarkable 23% overall yield. The synthesis of Zhang and colleagues also exemplifies how the inclusion of C–H oxidation reactions as a key part of synthesis planning can prompt the development of new methodologies and provide insight into the factors controlling site-selectivity.

Directed type 2 C–H oxidation

Type 2 C–H oxidations have been most commonly applied in directed functionalizations owing to greater development of these methodologies and the fact that the directing group often contains the heteroatom that is incorporated in the resulting heterocycle. These reactions have been pivotal in many recent syntheses of neurotropic sesquiterpenes[74], such as the synthesis by Shenvi and co-workers[87] of the sesquiterpene picrotoxinin[88] (**39**), which uses a directed type 2 C–H oxidation to form the C-2 to C-15 lactone (Fig. 5a). This oxidation-based transformation is more simple than traditional lactonizations as it reduces the number of functional groups one must install or carry through a given synthesis (Fig. 5b).

The Shenvi synthesis commenced with an unconventional strategic decision (Fig. 5c), beginning from dimethyl carvone (**46**), despite needing only one of the geminal methyl groups in the target natural product. This starting point was necessary to impart high levels of diastereoselectivity in an aldol reaction of **46** with ketone **47** to give the desired α-epimer of **48** in 67% yield. However, it required the extraneous methyl group to be removed later in the synthesis. A two-step annulation sequence delivered bicycle **49**, and the secondary hydroxy and *iso*-propenyl groups were protected through a bromoetherification reaction with NBS, affording **50** in near-quantitative yield. Conventional oxidation methodologies were used to install the lactone moiety

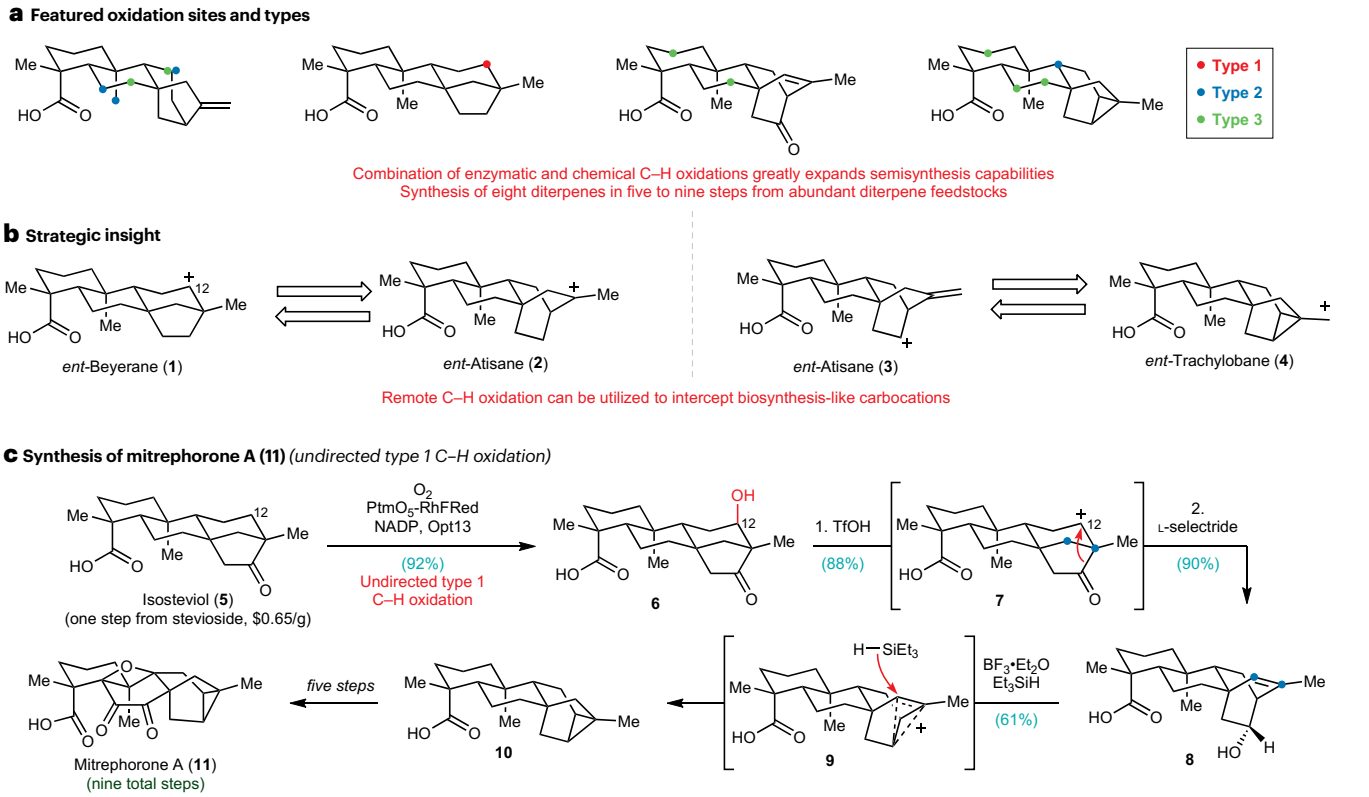

Fig. 2 | Syntheses of complex diterpenes featuring multiple C–H oxidations of terpene feedstocks by Renata and co-workers. a, Site and type of oxidations featured in the synthesis. **b**, Carbocationic relationship between bridged diterpenes. **c**, Synthesis of mitrephorone A (**11**) by Renata and colleagues features a type 1 C–H oxidation.

in **51**. A Suárez etherification mediated by the axially disposed secondary hydroxy group using AgOAc, I_2 and visible-light irradiation gave ether **52** through a selective 1,5-HAT, which was primed for a subsequent three-step oxidation, radical ring opening–halogenation and dehalogenation sequence to delete the additional methyl group, constituting an unconventional use of type 1 directed C–H oxidation. With the extra methyl removed, the synthesis was completed by directed type 2 C–H oxidation with $Pb(OAc)_2$, $CaCO_3$ and light to effect lactonization followed by reductive cleavage of the bromoether to give picrotoxinin (**39**) in 13 total steps — the shortest synthesis of this natural product to date[89–96].

The key to the efficacy of this synthesis was the use of dimethyl carvone as a starting material. The two methyl groups were installed in a single step and enabled a key diastereoselective annulation, even though neither appear at the methyl oxidation state in the natural product. One was deleted through a type 1 C–H oxidation, exemplifying how unactivated carbon substituents can now be conceptualized as removable auxiliary functionalities, and the other was converted into a heterocyclic structural element with a type 2 C–H oxidation, serving as a latent functional handle.

Type 3 C–H oxidation

Type 3 oxidations are those that introduce peripheral oxidation en route to a target natural product. These represent the most widely adopted use of C–H oxidation in synthesis and have proven to be a powerfully enabling strategy for late-stage diversification[97,98]. Type 3 oxidation can be conceptualized as a bioinspired approach, mimicking the two-phase biosynthetic logic found in terpenoid biosynthesis[26], in which promiscuous oxygenases are responsible for converting unfunctionalized metabolites to their higher-oxidation level congeners. This approach naturally leads to syntheses that are step-economic and limits protecting group manipulations or functional group interconversions by introducing sensitive functionality at a late stage. However, for two-phase synthetic approaches to be tenable, chemical methods for C–H oxidation must be on par with those of nature's, including an understanding of the principles that govern the selectivity in these reactions.

Undirected type 3 C–H oxidation

Many methods have been used that target the weakest electron-rich (hydridic) C–H bond in a given molecule, with some preferential targeting of secondary C–H bonds by using sterically bulky catalysts[12] (see Box 1). Other methodologies that target strong C–H bonds[99] and primary selective functionalization[100,101] have been developed but have not been used in total synthesis to date. As such, undirected type 3 oxidation methodologies have been predominantly used for targeting tertiary C–H bonds distal from electron-withdrawing groups, or proximal to electron-releasing groups. Several of the syntheses discussed in the previous sections include examples of undirected type 3 C–H oxidation — for more information, see the full papers from Renata et al.[50] and Zhang et al.[77].

An interesting case of selectivity was explored in the context of the total synthesis of *ent*-trachylobane[102] natural products by Magauer et al.[103] (Fig. 6). This work stands in juxtaposition to the biocatalytic C–H oxidations explored by Renata and colleagues (*vide supra*) and

highlights how the use of different methodologies can alter selectivity. To investigate chemical C–H oxidations, Magauer and co-workers targeted [3.2.1.0] tricycle **56**. Their synthesis commenced from decalin **53** that was accessed in eight steps from commercial material and was crucial in their prior synthesis of mitrephorone A (**11**) (Fig. 6a)[63]. A five-step sequence advanced **53** to enone **54**, which underwent Luche reduction and elimination with the Burgess reagent to give diene **55** in 30% yield over two steps. Diene **55** was primed for a key Diels–Alder

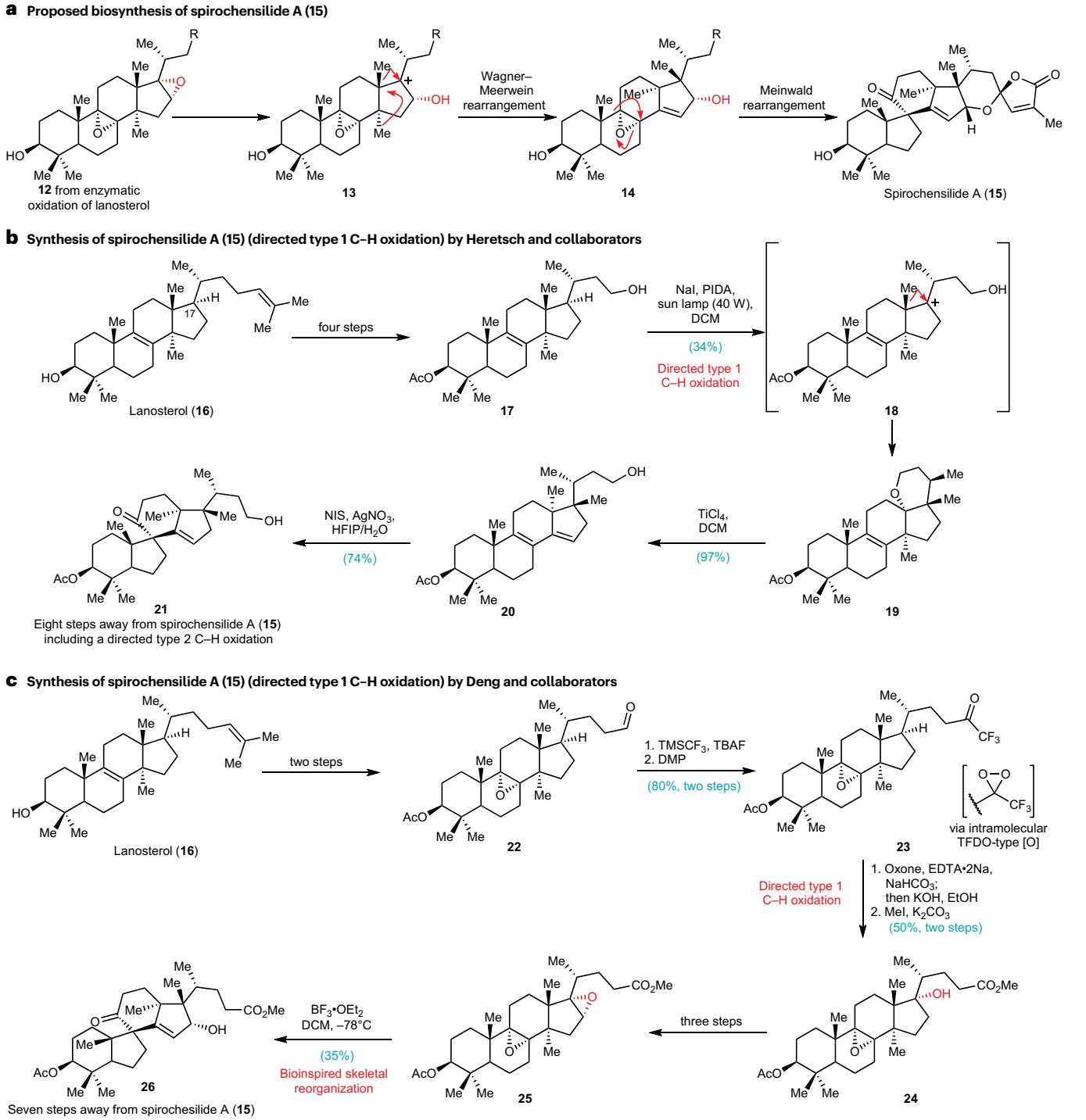

Fig. 3 | Syntheses of spirochensilide A starting from lanosterol by Heretsch et al. and Deng et al. a, The proposed biosynthesis of lanostane triterpenoid spirochensilide A (**15**) by Heretsch et al. and Deng et al. **b**,**c**, Heretsch and co-workers' (part **b**) and Deng and colleagues' (part **c**) syntheses of spirochensilide A (**15**) using directed type 1 C–H oxidation.

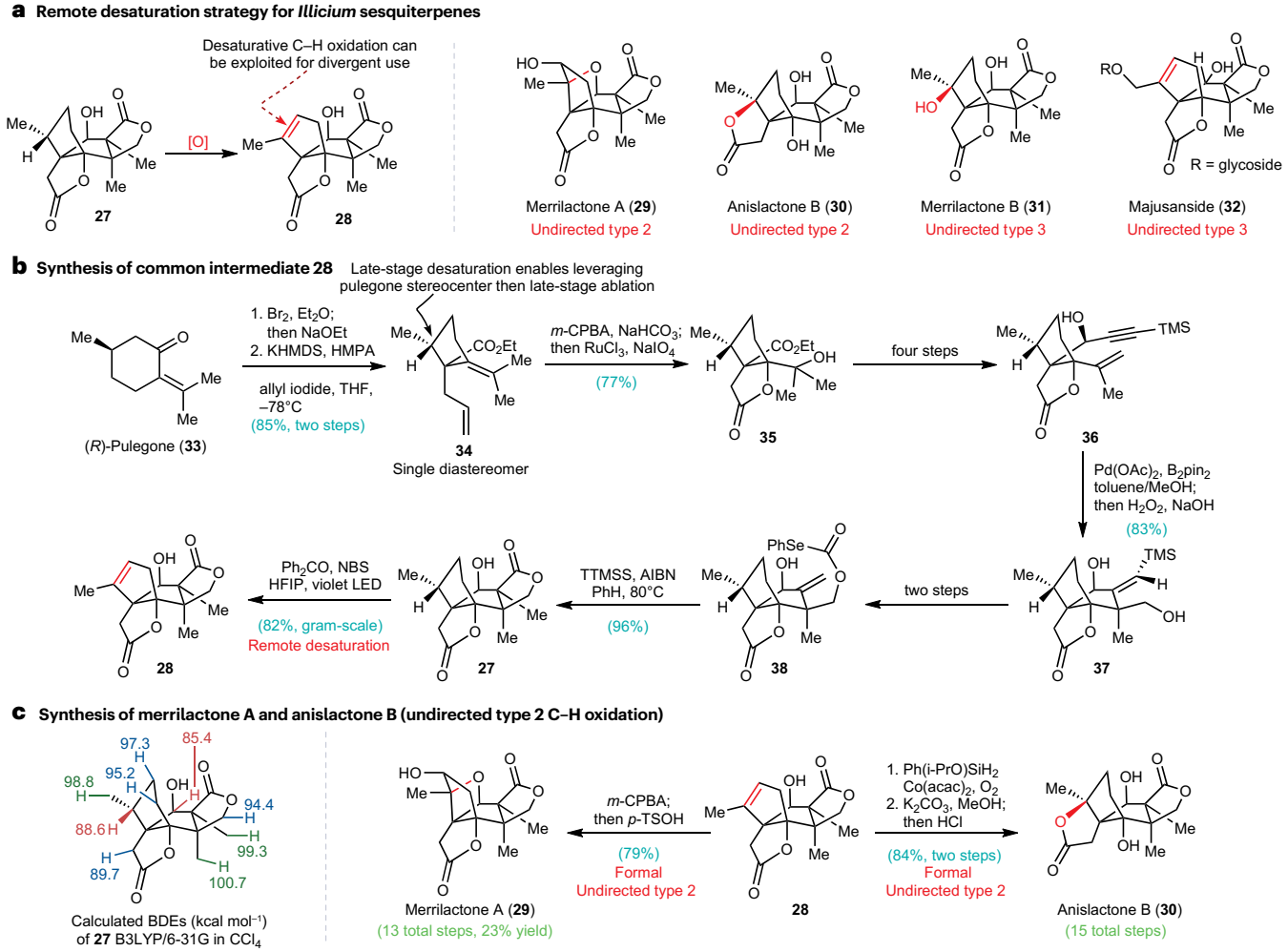

Fig. 4 | Synthesis of *Illicium* sesquiterpenes by Zhang et al. a, Remote desaturation plan to access several *Illicium* sesquiterpenes. **b**, Synthesis of the Zhang common intermediate through C–H oxidation. **c**, Completion of merrilactone A (**29**) and anislactone B (**30**) by leveraging desaturation for undirected type 2 C–H oxidation. BDE, bond dissociation energy.

cycloaddition, building the [3.2.1.0] tricycle of the family (see **56**) in 85% yield upon heating.

With the core of the trachylobanes assembled, Magauer et al. then explored the oxidation of its various structural elements (Fig. 6b). The use of the electrophilic oxidant methyl(trifluoromethyl)dioxirane (TFDO)[104,105] led to selective formation of **57** in 43% yield that afforded the corresponding natural product after ester saponification. The observed reactivity can be rationalized by the electron-releasing nature of the cyclopropane through hyperconjugation. Electrochemical oxidation[106] showed similar selectivity, but also gave 10% of the product corresponding to radical ring opening (not shown). The use of Ru(TMP)(CO)[107] also delivered the desired ketone in 27% yield and the lower-oxidation level alcohol in 38% yield. Selectivity was altered by using the bulky (*R*,*R*)-Mn(CF_3-PDP) catalyst[108] that resulted in the formation of **61**, containing the [2.2.2] bicycle that is characteristic of the *ent*-atisane natural products. This is presumably formed by oxidation at C-15 and subsequent radical ring opening.

The Magauer synthesis exemplifies how the analysis of substrate electronics is crucial for the successful application of undirected C–H oxidation methodology in synthesis planning, using the inherent – and atypical – structural features of their target to their advantage. A prior study by Chen and Baran has shown that ^{13}C-NMR shifts can be reliable predictors of site-selectivity[29], and Zhang and colleagues' synthesis of the *Illicium* sesquiterpenoids (*vide supra*) used BDE calculations to guide their planning.

Directed type 3 C–H oxidation

The utility of directed type 3 oxidation is demonstrated by Luan and colleagues'[109] elegant synthesis of dalesconol A[110] (Fig. 7a, **68**). This polyketide natural product contains three benzylic ketones with *ortho*-oxidation leading very naturally to the use of directed C–H oxidation for late-stage manipulations using the innate ketone functionalities – or derivatives thereof – as directing groups[111]. The researchers cleverly planned to perform all three oxidations in a single operation[112], thus rapidly installing the desired oxidation in a step-economic fashion. Additionally, this approach enabled the use of more simple starting materials, less prone to the interference of additional functionality with downstream chemistry and requiring fewer steps to prepare.

The Luan synthesis constructed the core of dalesconol A through a remarkably efficient Pd(0)-norbornene mediated Catellani-type cascade[113,114]. Aryl iodide **62** was coupled with alkyne **63** through activation of a C–H bond and migratory insertion across the alkyne, and the key spiro-tricycle was then formed through a one-pot ketal cleavage–Michael addition to give **64** in 64% yield. Benzylic oxidation of diketone **64** then gave triketone **65**, primed for the triple-directed type 3 oxidation. Although one-step trihydroxylation[115] directly from the ketone was unsuccessful, many alternative methods for ketone (or ketone-derivative)-directed C–H oxidations have been reported — an important consideration made by Luan et al. in their synthesis planning. Triketone **65** was converted to the corresponding trioxime methyl ether (**66**) in 88% yield by treatment with $MeONH_2HCl$. The oxime ethers were found to be suitable directing groups for the aromatic trihydroxylation reaction, installing all three hydroxy groups of the natural product in a single step[116]. The oximes were cleaved in situ upon addition of HCl, giving triol **67** in 41% yield, which is a remarkably high yield given that the three oxidations and directing group cleavages occurred in a single operation. This rapid increase in oxidation level clearly shows how judicious synthesis planning can enable highly efficient multiple operations. Advanced intermediate **67** was converted to dalesconol A (**68**) using a palladium-catalysed oxidation developed by Stahl and Diao[117] to complete the synthesis in a longest linear sequence of eight steps. The researchers also highlighted the power of their strategy for late-stage diversification wherein triketone **65** was sulfaminated using iridium catalysis[118] to give trisulfonamide **70** in 84% yield (Fig. 7b). The tosyl groups were cleaved with sulfuric acid to give the aminated analogue of dalesconol A (**71**) in 98% yield. The ease with which they were able to prepare these analogues is a strong argument for delaying the oxidation step as late as possible into the synthesis campaign — in this way, diverse libraries can be produced in the fewest possible steps.

Longiborneol sesquiterpenoids

Our own laboratory has had a long-standing interest in the application of C–H oxidation reactions to natural product synthesis. Below, we discuss our work towards the longiborneol and cephanolide–ceforalide natural products using a variety of C–H oxidation strategies (Fig. 8). The longiborneol sesquiterpenoid family[119–125] features 11 natural products, differing only in their positions of oxygenation around a common carbon framework. We saw the syntheses of these molecules as an ideal opportunity to showcase the power of Type 3 C–H oxidations for enabling divergent syntheses by accessing the more oxygenated congeners of longiborneol from the parent natural product longiborneol (**72**) or a derivative (see **73**, Fig. 8a). This key strategic decision would be coupled with a concise synthesis of longiborneol, using functionalized camphor intermediate **74** that was accessed through a scaffold remodelling approach of carvone (**75**) previously developed by our group[126,127]. Notably, this two-phase strategy enables the individual routes to diverge at the latest possible juncture, minimizing the total step count. Although we were unable to implement all the directed Type 3 C–H oxidations depicted in **73**, our investigations revealed current methodological gaps in the C–H oxidation literature, prompting us to develop new approaches. Ultimately, we were able to oxidize every targeted position with a mixture of directed and undirected methods, which we hope will serve as proof-of-concept studies for future investigations on related scaffolds.

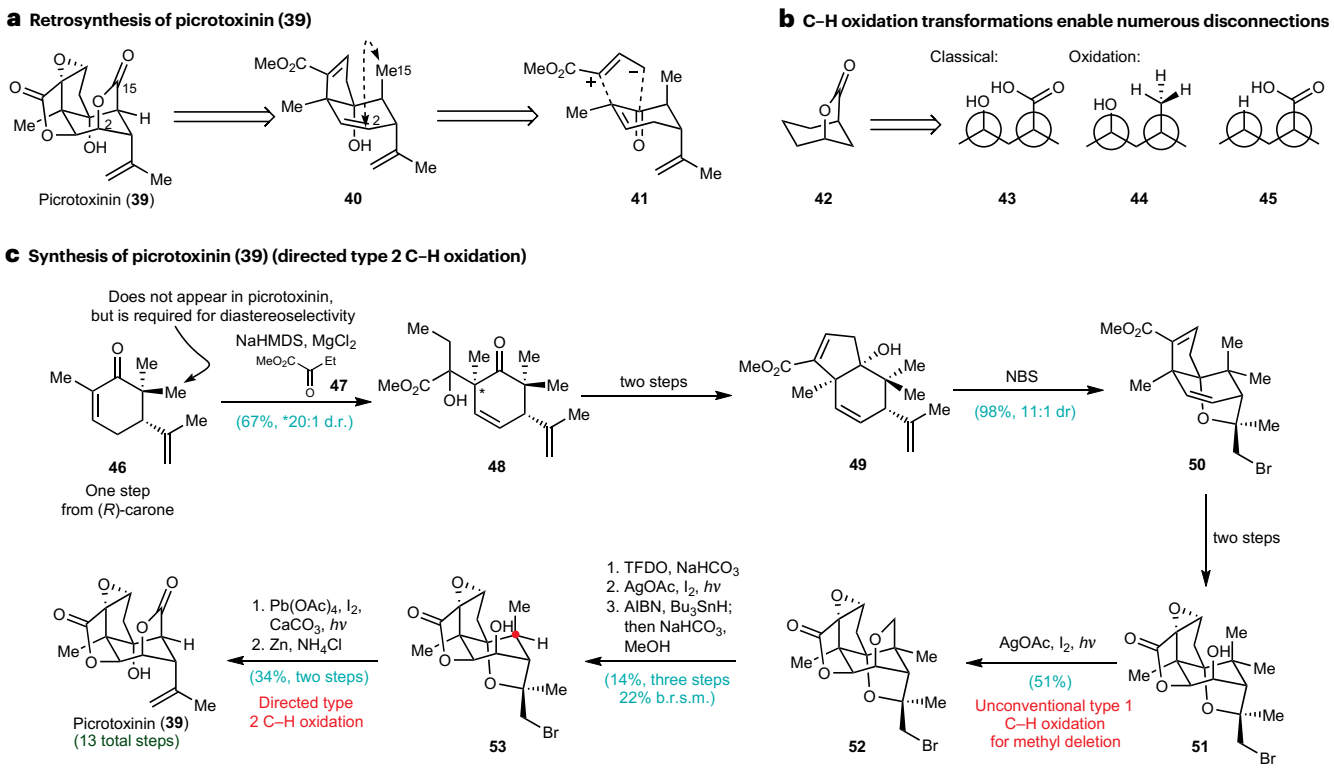

Fig. 5 | Synthesis of picrotoxinin by Shenvi et al. a, Retrosynthesis of picrotoxinin by Shenvi and colleagues. **b**, Oxidation-based lactonization disconnections compared to classical disconnection. **c**, Synthesis of picrotoxinin featuring a type 2 directed C–H oxidation. b.r.s.m., based on recovered starting material; d.r., diastereometric ratio.

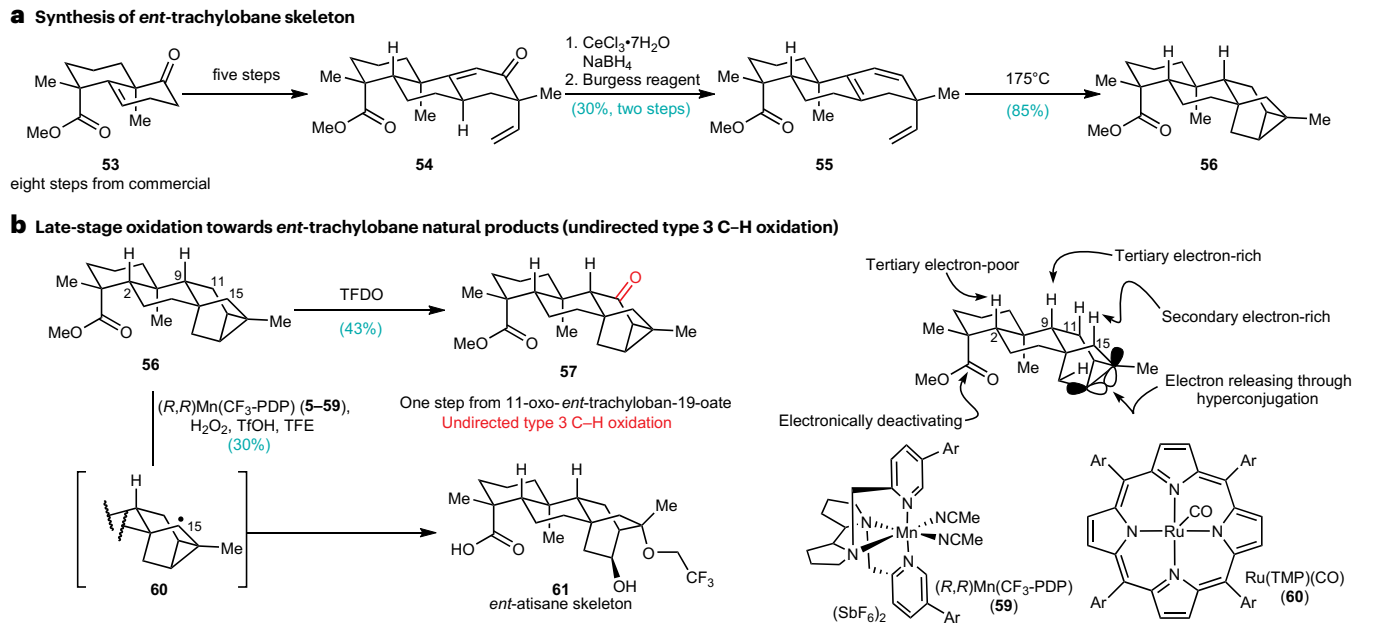

Fig. 6 | Synthesis of *ent*-trachylobane natural products by Magauer et al. a, Synthesis of the *ent*-trachylobane skeleton. **b**, Undirected type 3 C–H oxidation towards *ent*-trachylobane natural products. The C=O highlighted red in **b** indicates that it was installed via the TFDO-mediated C–H oxidation reaction.

We commenced with the synthesis of common intermediate **76** from (*S*)-carvone (**75**) in seven steps (Fig. 8b). Longiborneol (**72**) was synthesized from tricycle **76** by hydrogenation of the alkene group and dissolving metal reduction of the carbonyl group. Following acetylation of longiborneol to give **77**, we targeted the C-11 oxidized congeners, culmorone (**78**) and culmorin (**79**), through an undirected type 3 strategy. We expected acetylation would deactivate C-8–H towards certain type 3 C–H oxidations[128]. Although we hypothesized that oxidation of **77** with TFDO or the White–Chen catalyst would result primarily in oxidation at C-4 — the most sterically accessible methylene group[12] — we also anticipated oxidation at C-11 to occur as a result of strain acceleration[105] and the fact that C-11 is the only other non-neopentyl methylene. In fact, oxidation of **77** with TFDO did lead to C-4 and C-11 oxidized products, but yields were low and minor side-products (oxidation at C-5 and C-3) were also observed (not pictured). Despite these shortcomings, the high overall yield of **77** from carvone meant that we were still able to obtain synthetically useful amounts of the C-11 oxidized products. Cleavage of the acetate group yielded culmorone (**78**) and subsequent dissolving metal reduction gave culmorin (**79**).

Next, we investigated whether the installation of additional functionality could enable the use of the TFDO type 3 C–H oxidation in a more selective synthesis of 5-hydroxyculmorin (**80**) from a 5-hydroxylongiborneol derivative (Fig. 8c). Allylic oxidation of **76** was used to install a hydroxy group at C-5. Subsequent alkene hydrogenation and carbonyl reduction gave 5-hydroxylongiborneol (**81**). Acetylation of both hydroxy groups furnished **82**, which underwent selective TFDO-mediated oxidation at C-11 owing to deactivation at C-5, C-4 and C-3 by the inductively electron-withdrawing C-5 acetate, affording C-11 ketone **83** as the only observed product. Treatment with dissolving metal conditions cleaved both acetate esters and reduced the carbonyl group to give 5-hydroxyculmorin (**80**).

Directed type 3 oxidations were then used to target the additional positions on the longiborneol skeleton. Hydrogenation of **76** followed by reduction of the carbonyl group with $LiAlH_4$ gave C-8-epi-longiborneol, and subsequent treatment with dimethylchlorosilane yielded **84**. The (hydrido)silyl ether group of **84** was then used to direct a Hartwig silylation of C-12 via iridacycle **85**[129,130]. Tamao–Fleming oxidation of the resulting silacycle gave C-8-epi-12-hydroxylongiborneol that was converted to the natural product (**86**) by DMP oxidation of both hydroxy groups and reduction of the resulting carbonyls. Notably, attempts to implement a similar synthetic sequence from longiborneol (**72**) were ineffective, probably because of an unfavourable geometric relationship between the corresponding (hydrido) silyl ether and the C-12 methyl group. This outcome highlights the effects of conformation and geometry on the efficacy of directed C–H oxidation[131], a subtlety that is often not apparent or as pronounced in simpler substrates.

Similarly, our attempts to oxidize C-15 using a type 3 C–H oxidation directed by a functional group at C-8 were also ineffective. Attempts to use **84** in a Rh-catalysed Hartwig silylation[132], known to favour 1,4 functionalization in some cases, led only to C-12 functionalization, probably owing to a lack of steric differentiation between C-12 and C-15. An attempted Suárez reaction from C-8-epi-longiborneol (not pictured) led to a complex mixture, possibly owing to competitive β-scission of the [2.2.1] bicycle[133]. Again, these challenges highlight the need to consider many substrate characteristics — such as relative steric encumbrance and strain energy — when using C–H oxidation chemistry on complex molecules. As an alternative, we devised a relay oxidation strategy[134,135] in which a functional group installed at C-5 was used to direct the oxidations of C-14 and C-15. To implement this strategy, we synthesized acetyl oxime **87** in six steps from the common intermediate **76**. Treatment of **87** with modified Sanford acetoxylation conditions — $Pd(OAc)_2$ and sub-stoichiometric quantities of PIDA — resulted in a directed type 3 C–H oxidation of both C-14 and C-15 to give **88** as a 2:1 inseparable mixture of diastereomers[136], favouring the C-14 oxidized product. Reductive cleavage of the oxime[111], installation of a

tosyl hydrazone group and a $LiAlH_4$-mediated Caglioti reaction led to a separable mixture of the natural products 14-hydroxylongiborneol (**89**) and 15-hydroxylongiborneol (**90**).

The studies described in the previous sections provided insight into the application of the Sanford acetoxylation chemistry. First, the steric environment of the ketone precursor requires careful consideration for the identity of the oxime and the method of its installation. Second, even if a given oxime is a competent directing group, challenges in cleaving the oxime can be prohibitive for practical application. For example, we found hydrolysis of the analogous methoxime derivative of **88** to be challenging. Successful examples in complex molecule synthesis generally require harsh, acidic conditions[137,138], and few other conditions for methoxime cleavage have been reported[139]. Conversely, the one-pot procedure used in our work allows for installation of an acetyl oxime in a single step, which can be cleaved under milder conditions[140]. Finally, in targeting mono-oxidation of a gem-dimethyl group, bis-acetoxylated products can be expected in the absence of conformational rigidity. For example, **87** → **88** required sub-stoichiometric PIDA to slow the formation of bis-acetoxylated products at C-14 and C-15.

In summary, we used a diverse array of type 3 C–H oxidations to access seven oxidized longiborneol congeners, which collectively feature oxidation at five distinct sites on the natural product skeleton. Our use of C–H oxidation chemistry enabled each of these syntheses to begin from the common intermediate **76**, which features the complete carbon skeleton and only two functional groups. This two-phase strategy reflects the synthetic promise of type 3 oxidations in enabling the synthesis of multiple targets through the step-efficient late-stage diversification of synthetically advanced common intermediates.

Cephalotane norditerpenoids

Another example that underscores the power of late-stage C–H oxidations is our divergent total syntheses of C-18-benzenoid and C-19-benzenoid cephalotane-type norditerpenoids[35,40] (Fig. 9). These molecules have also attracted significant synthetic interest from the Zhao, Gao, Cai, Zhang, Zhai and Hu groups[141–149]. In our retrosynthesis, we identified **91**, bearing the benzenoid cephalotane core ring system, as the optimal common intermediate for late-stage diversification. On the basis of the maximally bridged ring[150–152], we found the depicted two-bond inverse-electron-demand Diels–Alder-type disconnection to be appealing for rapid simplification of the core structure (Fig. 9a, **92**). We envisioned **92** arising through an iterative Suzuki cross-coupling of indanone-triflate **93** and pyrone-triflate **95** with BF_3K–ethylene–9BBN (**94**)[153].

Our syntheses commenced with 7-hydroxy-4-methyl-indanone, which was converted to indanone-pyrone **92** in three steps. Subsequent inverse-electron-demand Diels–Alder-type cycloaddition proceeded smoothly upon enoxy-silylation to give **91** as a single diastereomer (Fig. 9b). Borocupration of the alkene[154,155] and addition of MeI as an electrophile gave access to boron pinacol ester **99**, which underwent either protodeboronation[156] to afford **98** or a one-pot oxidation to alcohol **96**. We then sought to apply type 2 and type 3 C–H oxidations to diversify these key intermediates to the targeted natural products. Following $InCl_3$-catalysed ionic deoxygenation[157,158] of **98**, undirected

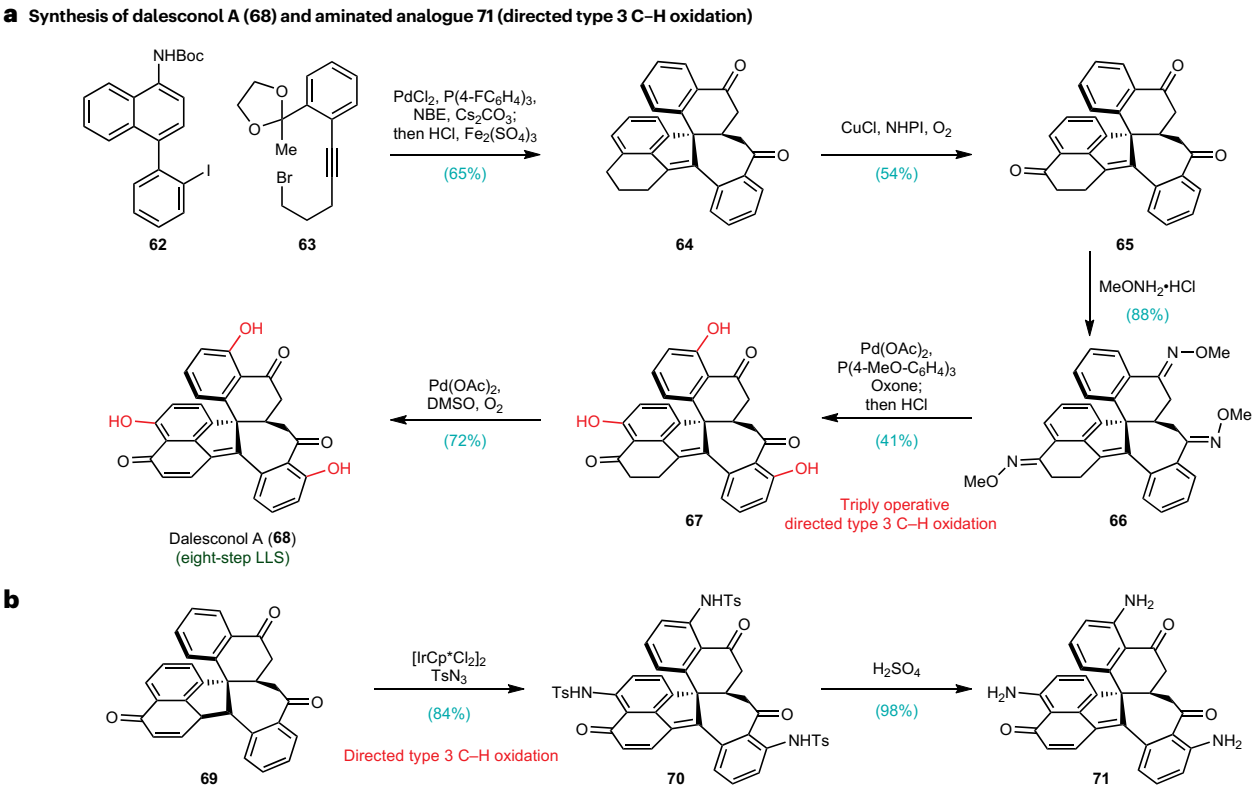

Fig. 7 | Synthesis of dalesconol A by Luan et al. a, Forward synthesis of dalesconol A, featuring multiple directed type 3 C–H oxidations in a single operation. **b**, Use of directed type 3 C–H oxidation to access dalesconol A analogues. LLS, longest linear sequence.

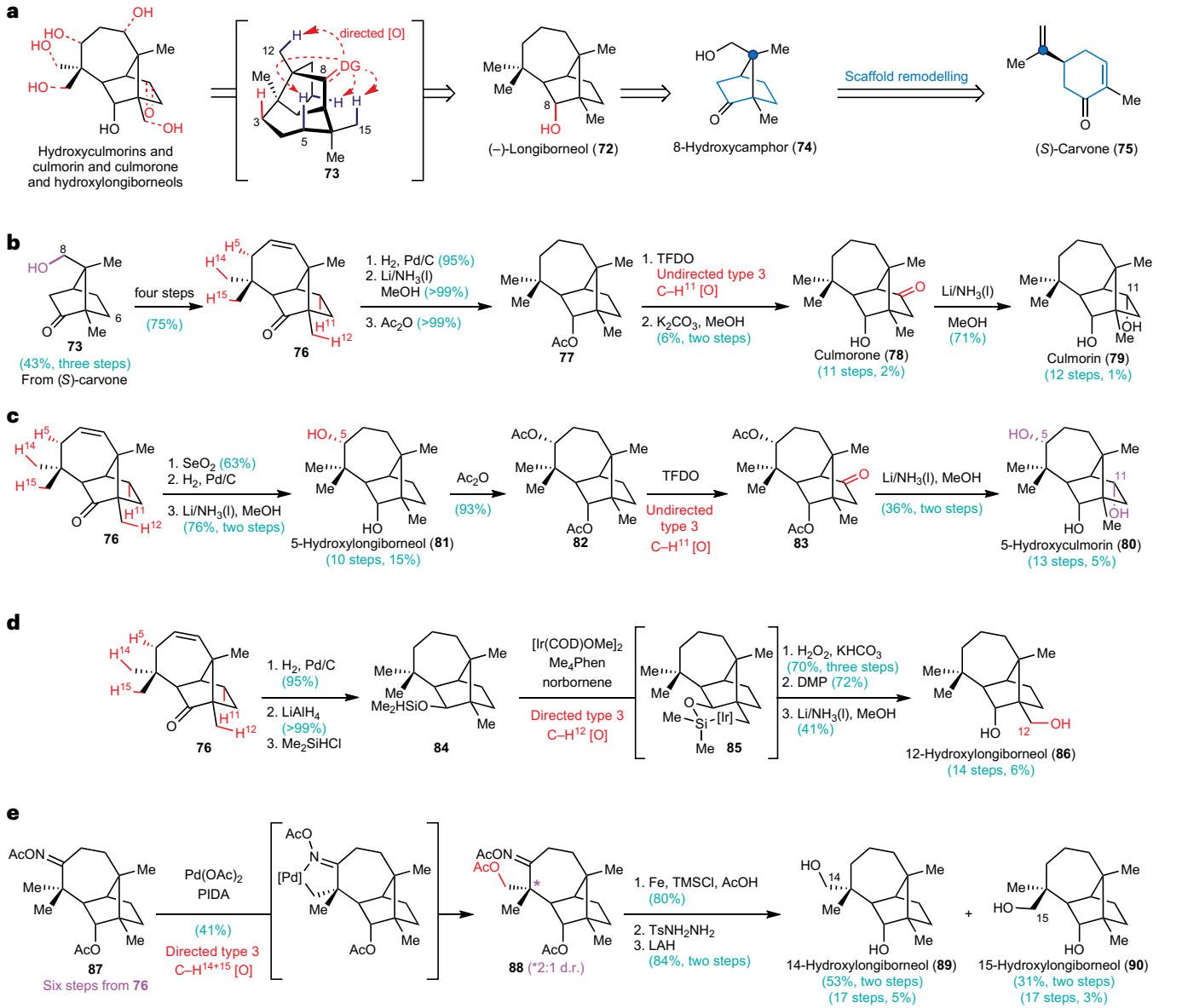

Fig. 8 | Synthesis of longiborneol sesquiterpenes by Sarpong and co-workers. **a**, Two-phase retrosynthesis of longiborneol (**72**) sesquiterpenoids. **b**–**e**, Syntheses of culmorone and culmorin (**b**), 5-hydroxyculmorin (**c**), 12-hydroxylongiborneol (**d**) and 14- and 15-hydroxiborneol (**e**) using both directed and undirected type 3 C–H oxidations. d.r., diastereometric ratio. The colours indicate the positions targeted for C–H oxidation and functional groups installed using C–H functionalization.

type 3 C–H oxidation of the aryl ring under mild conditions with phthaloyl peroxide[159] afforded cephanolide B (**103**) as a 1.3:1 mixture with its C-15-oxidized constitutional isomer. Alternatively, thianthrenation conditions[160] developed in the Ritter group, followed by subsequent borylation and oxidation, gave the C-13-oxidized and C-15-oxidized products as a 1:1 mixture in a one-pot (67%) procedure, or a higher yielding two-step procedure (94%). We hypothesize that the low observed selectivity arises from both positions being electronically and sterically similar. Cephanolide C (**105**) was accessible through an undirected benzylic oxidation of intermediate **98** with pyridinium chlorochromate. Installation of a methoxime facilitated a directed type 1 C–H methoxycarbonylation[161] using stoichiometric amounts of $Pd(OAc)_2$ to afford methyl ester **109**. As observed in our longiborneol work (*vide supra*), cleavage of the methyloxime was challenging and ozonolysis[162] proved uniquely effective to yield cephanolide D (**110**).

Next, we targeted ceforalide C, D and F from alcohol **96** (*vide supra*). A four-step sequence afforded ceforalide D (**100**) through inversion of the alcohol and deoxygenation of the protected tertiary hydroxy group. Furthermore, selective undirected benzylic oxidation using $Ru(bpy)_3Cl_2$ as a photocatalyst, a hydroxyl benziodoxole hypervalent iodine reagent (BI-OH)[163] and 400 nm irradiation gave ceforalide C (**106**) in the presence of the unprotected hydroxy group

of ceforalide D (**100**). Type 2 C–H oxidation was then applied to access ceforalide F (**107**) from ceforalide D (**100**), closing the THF ring with modified Suárez oxidation conditions ($Pb(OAc)_4$, I_2 and $CaCO_3$ under fume hood light), followed by pyridinium chlorochromate-mediated benzylic oxidation of C-7.

To access cephanolide A (**104**), DMP oxidation of alcohol **96**, followed by treatment with $NaBH_4$, inverted the hydroxy group. This set the stage for a directed type 2 Suárez oxidation (with PIDA and I_2)[75] to forge the THF ring, and subsequent one-pot cleavage of the TMS ether with tetrabutylammonium fluoride. Barton–McCombie deoxygenation delivered hexacycle **101**. In contrast to the analogous transformation towards cephanolide B (**103**) (*vide supra*), C–H thianthrenation proceeded in quantitative yield and high selectivity (13:1). Calculations revealed a higher electrostatic potential at C-13 than at C-15 in precursor **101** than in precursor **98**, rationalizing the observed selectivity. An altered steric environment owing to conformational changes induced by the additional THF ring may also factor into the selectivity. Subsequent conversion to the corresponding Bpin compound (**108**) under photoirradiation conditions and direct one-pot oxidation efficiently furnished cephanolide A (**104**), constituting an overall undirected type 3 oxidation. Finally, ceforalide G (**111**) was targeted through an overall undirected type 3 oxidation. Undirected benzylic oxidation of Bpin

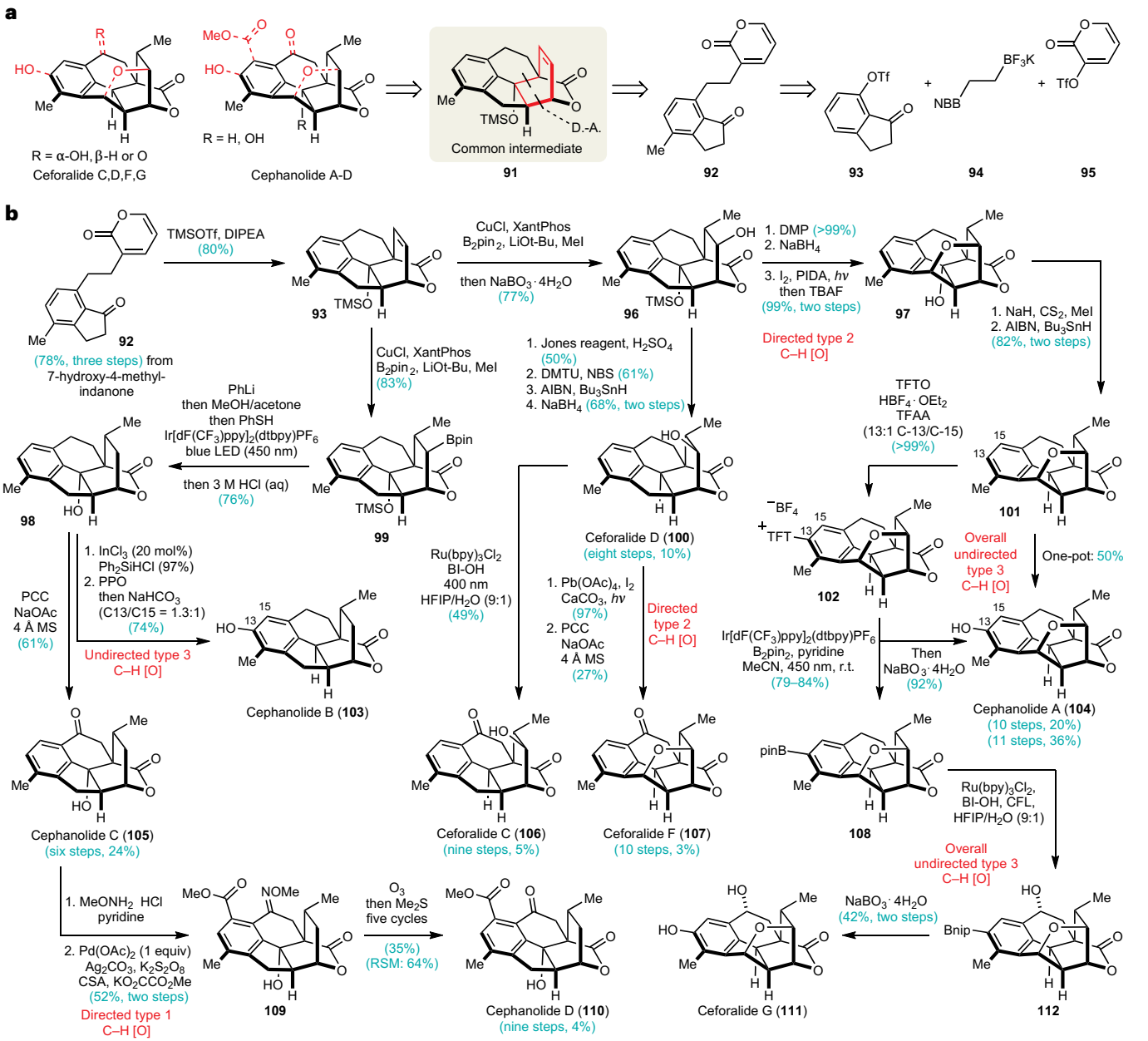

Fig. 9 | Synthesis of cephalotane norditerpenoids by Sarpong and co-workers. a, Retrosynthesis of cephalotane-type norditerpenoids. **b**, Unified total syntheses of cephalotane-type norditerpenoids using several different types of C–H oxidations. CFL, compact fluorescent lamp; MS, molecular sieve.

compound (**108**) under photoredox conditions using $Ru(bpy)_3Cl_2$, BI-OH and a compact fluorescent lamp, followed by oxidation of the Bpin group to the corresponding hydroxy group, gave the natural product **111**. Notably, all other alternatives to the specified sequence of oxidation steps from **101** towards ceforalide G (**111**) were unsuccessful.

Overall, we were able to access nine cephanolide–ceforalide-type natural products (ceforalide H is not shown) through the application of type 2 and type 3 C–H oxidations of a common synthetic precursor. Notably, many of these transformations rely on contemporary methods. For example, to the best of our knowledge, this work constitutes the first application of the Ritter thianthrenation chemistry in total synthesis, highlighting how methodological development can be an enabling and motivating factor in synthesis planning.

Conclusion and outlook

The strategic application of C–H oxidation in natural product total synthesis is increasingly being incorporated at the outset of synthesis planning. To guide future synthetic endeavours that utilize C–H oxidation, we propose the classifications of these applications of C–H oxidation on the basis of their overall strategic purpose with respect to the target natural product.

Type 1 C–H oxidations establish the target molecule's carbon skeleton by leveraging the oxidation to construct, cleave or rearrange the C–C bonds of an intermediate. This enables strategies in which relatively large, structurally complex chiral pool feedstock chemicals can be utilized as starting materials in syntheses of target molecules they do not directly map into. Such approaches often reduce step counts compared to strategies in which the carbon skeleton is built additively. Such C–H oxidations are relatively uncommon and tend to be seen in the early stages of syntheses. As such, the oxidation reactions need to be robust and highly scalable. On the basis of the approaches demonstrated by Renata, Deng, Heretsch and colleagues, we expect that strategies centred on type 1 C–H oxidations will continue to develop rapidly. Although bioinspired carbocation rearrangements have proven particularly effective, in the future, we anticipate that C–H oxidation will also be leveraged to install handles for C–C bond formation or cleavage, enabling synthesis connections between disparate natural product scaffolds and the recognition of new or underutilized chiral pool feedstocks as valuable starting materials for total synthesis.

Type 2 C–H oxidations ultimately result in the formation of a heterocyclic ring found in the target natural product. Introducing remote functionalization to construct the ring minimizes functional group interconversion and protects group manipulations. We anticipate that further applications will benefit from the development of C–H oxidation methodologies capable of achieving more varied site-selectivity. Specifically, directed approaches have mainly focused on the formation of five-membered oxygen-containing heterocycles that incorporate the directing functionality and undirected approaches are limited.

Type 3 C–H oxidations install requisite peripheral functionalization present in the target and represent the ultimate goal of late-stage functionalization: to rapidly assemble a natural product core without the complications associated with preinstalled functionality, then diversify to synthesize many desired compounds through site-selective C–H oxidation. Further methodological developments will increase the success rate of late-stage functionalization. Strategies that utilize supramolecular control to override site-selectivity have tremendous promise especially in the area of biocatalysis, which may lead, excitingly, to evolvable site-selectivity.

It is our expectation that undirected C–H oxidations and type 1 C–H oxidation-based strategies will be more commonly used in the future than they are at present. Currently, directed C–H oxidations are often superior to undirected variants in controlling site-selectivity. However, the installation and removal of directing groups can be challenging and also add steps to a synthesis. As undirected methods become more robust and tunable, through paradigms such as biocatalysis, we expect their usage in synthesis to increase. Of the three types of C–H oxidation-based strategies, type 2 and 3 strategies are currently more prevalent than type 1. Reactions involving C–H oxidation often convert a C–H bond into an oxygenated functional group, and so it is easy to recognize, in the retrosynthetic direction, the deletion of a functional group to give a synthetically more tractable precursor. However, the examples both in this Review and others have shown that type 1 C–H oxidations can be used to remodel the carbon skeleton of a starting material to match the framework of the target. These strategies are less intuitive but are powerful because they effectively expand the pool of starting materials that can be applied to a given target. As the available C–H oxidation methodologies continue to expand, increasing the number of examples from which practitioners can draw inspiration, we anticipate that type 1 strategies will become more common.

Together, we hope that the framework for categorizing C–H oxidation strategies in complex molecule synthesis presented in this Review will guide future synthesis planning, aid discussion and help facilitate entry into this field. It is our hope that this classification system will help move C–H oxidation reactions from exotic highlights of a synthesis to routine synthetic tools. This shift could accelerate the application of contemporary methodologies in total synthesis, which will be crucial in gaining a comprehensive understanding of the factors that lead to the success or failure of such transformations, particularly concerning site-selectivity. In turn, applications in complex molecule synthesis should motivate and accelerate new methodological investigations. Therefore, we anticipate that many more innovative syntheses (like those discussed in this Review) that strategically apply C–H oxidation will continue to emerge. Finally, we hope that viewing the use of C–H oxidation in natural product synthesis through our classification system will inspire less intuitive applications of C–H oxidation.

Published online: 20 September 2023

References

1. Yamaguchi, J., Yamaguchi, A. D. & Itami, K. C–H bond functionalization: emerging synthetic tools for natural products and pharmaceuticals. *Angew. Chem. Int. Ed. Engl.* **51**, 8960–9009 (2012).
2. Davies, H. M. L. & Morton, D. Recent advances in C–H functionalization. *J. Org. Chem.* **81**, 343–350 (2016).
3. Rogge, T. et al. C–H activation. *Nat. Rev. Methods Primers* **1**, 1–31 (2021).
4. Davies, H. M. L., Bois, J. D. & Yu, J.-Q. C–H functionalization in organic synthesis. *Chem. Soc. Rev.* **40**, 1855–1856 (2011).
5. Bellina, F. & Rossi, R. Transition metal-catalyzed direct arylation of substrates with activated sp^3-hybridized C–H bonds and some of their synthetic equivalents with aryl halides and pseudohalides. *Chem. Rev.* **110**, 1082–1146 (2010).
6. Che, C.-M., Lo, V. K.-Y., Zhou, C.-Y. & Huang, J.-S. Selective functionalisation of saturated C–H bonds with metalloporphyrin catalysts. *Chem. Soc. Rev.* **40**, 1950–1975 (2011).
7. Zhou, M. & Crabtree, R. H. C–H oxidation by platinum group metal oxo or peroxo species. *Chem. Soc. Rev.* **40**, 1875–1884 (2011).
8. Lu, H. & Zhang, X. P. Catalytic C–H functionalization by metalloporphyrins: recent developments and future directions. *Chem. Soc. Rev.* **40**, 1899–1909 (2011).
9. Guo, X.-X., Gu, D.-W., Wu, Z. & Zhang, W. Copper-catalyzed C–H functionalization reactions: efficient synthesis of heterocycles. *Chem. Rev.* **115**, 1622–1651 (2015).
10. Gensch, T., Hopkinson, M. N., Glorius, F. & Wencel-Delord, J. Mild metal-catalyzed C–H activation: examples and concepts. *Chem. Soc. Rev.* **45**, 2900–2936 (2016).
11. Hartwig, J. F. Catalyst-controlled site-selective bond activation. *Acc. Chem. Res.* **50**, 549–555 (2017).
12. Gormisky, P. E. & White, M. C. Catalyst-controlled aliphatic C–H oxidations with a predictive model for site-selectivity. *J. Am. Chem. Soc.* **135**, 14052–14055 (2013).

13. Zhang, Q. & Shi, B.-F. Site-selective functionalization of remote aliphatic C–H bonds via C–H metallation. *Chem. Sci.* **12**, 841–852 (2021).
14. Christmann, M. Selective oxidation of aliphatic C–H bonds in the synthesis of complex molecules. *Angew. Chem. Int. Ed. Engl.* **47**, 2740–2742 (2008).
15. Gutekunst, W. R. & Baran, P. S. C–H functionalization logic in total synthesis. *Chem. Soc. Rev.* **40**, 1976–1991 (2011).
16. McMurray, L., O'Hara, F. & Gaunt, M. J. Recent developments in natural product synthesis using metal-catalysed C–H bond functionalisation. *Chem. Soc. Rev.* **40**, 1885–1898 (2011).
17. Newhouse, T. & Baran, P. S. If C–H bonds could talk: selective C–H bond oxidation. *Angew. Chem. Int. Ed. Engl.* **50**, 3362–3374 (2011).
18. Chen, D. Y.-K. & Youn, S. W. C–H activation: a complementary tool in the total synthesis of complex natural products. *Chem. Eur. J.* **18**, 9452–9474 (2012).
19. Qiu, Y. & Gao, S. Trends in applying C–H oxidation to the total synthesis of natural products. *Nat. Prod. Rep.* **33**, 562–581 (2016).
20. Karimov, R. R. & Hartwig, J. F. Transition-metal-catalyzed selective functionalization of C(sp^3)–H bonds in natural products. *Angew. Chem. Int. Ed. Engl.* **57**, 4234–4241 (2018).
21. Abrams, D. J., Provencher, P. A. & Sorensen, E. J. Recent applications of C–H functionalization in complex natural product synthesis. *Chem. Soc. Rev.* **47**, 8925–8967 (2018).
22. Santana, V. C. S., Fernandes, M. C. V., Cappuccelli, I., Richieri, A. C. G. & de Lucca Jr, E. C. Metal-catalyzed C–H bond oxidation in the total synthesis of natural and unnatural products. *Synthesis* **54**, 5337–5359 (2022).
23. Trost, B. M. Selectivity: a key to synthetic efficiency. *Science* **219**, 245–250 (1983).
24. King, S. M. & Herzon, S. B. Substrate-modified functional group reactivity: hasubanan and acutumine alkaloid syntheses. *J. Org. Chem.* **79**, 8937–8947 (2014).
25. Green, S. A. et al. The high chemofidelity of metal-catalyzed hydrogen atom transfer. *Acc. Chem. Res.* **51**, 2628–2640 (2018).
26. Ishihara, Y. & Baran, P. S. Two-phase terpene total synthesis: historical perspective and application to the Taxol® problem. *Synlett* **2010**, 1733–1745 (2010).
27. Kanda, Y. et al. Two-phase synthesis of Taxol. *J. Am. Chem. Soc.* **142**, 10526–10533 (2020).
28. Kanda, Y., Ishihara, Y., Wilde, N. C. & Baran, P. S. Two-phase total synthesis of taxanes: tactics and strategies. *J. Org. Chem.* **85**, 10293–10320 (2020).
29. Chen, K. & Baran, P. S. Total synthesis of eudesmane terpenes by site-selective C–H oxidations. *Nature* **459**, 824–828 (2009).
A landmark synthesis using C–H oxidations in a two-phase approach.
30. Hung, K. et al. Development of a terpene feedstock-based oxidative synthetic approach to the *Illicium* sesquiterpenes. *J. Am. Chem. Soc.* **141**, 3083–3099 (2019).
A synthesis featuring several enabling C–H oxidations expanding the possibilities of chiral pool strategies.
31. West, S. P., Bisai, A., Lim, A. D., Narayan, R. R. & Sarpong, R. Total synthesis of (+)-lyconadin A and related compounds via oxidative C–N bond formation. *J. Am. Chem. Soc.* **131**, 11187–11194 (2009).
32. Fischer, D. F. & Sarpong, R. Total synthesis of (+)-complanadine A using an iridium-catalyzed pyridine C–H functionalization. *J. Am. Chem. Soc.* **132**, 5926–5927 (2010).
33. Newton, J. N., Fischer, D. F. & Sarpong, R. Synthetic studies on pseudo-dimeric lycopodium alkaloids: total synthesis of complanadine B. *Angew. Chem. Int. Ed. Engl.* **52**, 1726–1730 (2013).
34. Leal, R. A. et al. Application of a palladium-catalyzed C–H functionalization/indolization method to syntheses of *cis*-trikentrin A and herbindole B. *Angew. Chem. Int. Ed. Engl.* **55**, 11824–11828 (2016).
35. Haider, M., Sennari, G., Eggert, A. & Sarpong, R. Total synthesis of the *Cephalotaxus* norditerpenoids (±)-cephanolides A–D. *J. Am. Chem. Soc.* **143**, 2710–2715 (2021).
36. Haley, H. M. S. et al. Bioinspired diversification approach toward the total synthesis of lycodine-type alkaloids. *J. Am. Chem. Soc.* **143**, 4732–4740 (2021).
37. Jones, K. E., Park, B., Doering, N. A., Baik, M.-H. & Sarpong, R. Rearrangements of the chrysanthenol core: application to a formal synthesis of xishacorene B. *J. Am. Chem. Soc.* **143**, 20482–20490 (2021).
38. Lusi, R. F., Sennari, G. & Sarpong, R. Total synthesis of nine longiborneol sesquiterpenoids using a functionalized camphor strategy. *Nat. Chem.* **14**, 450–456 (2022).
39. Lusi, R. F., Sennari, G. & Sarpong, R. Strategy evolution in a skeletal remodeling and C–H functionalization-based synthesis of the longiborneol sesquiterpenoids. *J. Am. Chem. Soc.* **144**, 17277–17294 (2022).
A synthesis that combines skeletal remodeling of the chiral pool feedstock, carvone and late-stage C–H oxidations to access several longiborneol sesquiterpenoids.
40. Sennari, G. et al. Unified total syntheses of benzenoid cephalotane-type norditerpenoids: cephanolides and ceforalides. *J. Am. Chem. Soc.* **144**, 19173–19185 (2022).
A synthesis featuring a mix of aliphatic and aromatic C–H oxidations to access distinct natural product family members.
41. Perea, M. A. et al. General synthetic approach to diverse taxane cores. *J. Am. Chem. Soc.* **144**, 21398–21407 (2022).
42. Breslow, R. Biomimetic control of chemical selectivity. *Acc. Chem. Res.* **13**, 170–177 (1980).
A classic example of directed C–H oxidation using a tethered benzophenone group.
43. Lyons, T. W. & Sanford, M. S. Palladium-catalyzed ligand-directed C–H functionalization reactions. *Chem. Rev.* **110**, 1147–1169 (2010).
44. Mo, F., Tabor, J. R. & Dong, G. Alcohols or masked alcohols as directing groups for C–H bond functionalization. *Chem. Lett.* **43**, 264–271 (2014).
45. Gandeepan, P. & Ackermann, L. Transient directing groups for transformative C–H activation by synergistic metal catalysis. *Chem* **4**, 199–222 (2018).
46. Murali, K. et al. Decoding directing groups and their pivotal role in C–H activation. *Chem. Eur. J.* **27**, 12453–12508 (2021).
47. Hartwig, J. F. & Larsen, M. A. Undirected, homogeneous C–H bond functionalization: challenges and opportunities. *ACS Cent. Sci.* **2**, 281–292 (2016).
48. Brill, Z. G., Condakes, M. L., Ting, C. P. & Maimone, T. J. Navigating the chiral pool in the total synthesis of complex terpene natural products. *Chem. Rev.* **117**, 11753–11795 (2017).
49. Stout, C. N. & Renata, H. Reinvigorating the chiral pool: chemoenzymatic approaches to complex peptides and terpenoids. *Acc. Chem. Res.* **54**, 1143–1156 (2021).
50. Zhang, X. et al. Divergent synthesis of complex diterpenes through a hybrid oxidative approach. *Science* **369**, 799–806 (2020).
A chemoenzymatic synthesis featuring numerous strategically crucial C–H oxidations.
51. Hong, Y. J. & Tantillo, D. J. Formation of beyerene, kaurene, trachylobane, and atiserene diterpenes by rearrangements that avoid secondary carbocations. *J. Am. Chem. Soc.* **132**, 5375–5386 (2010).
52. Li, C. et al. A hexacyclic *ent*-trachylobane diterpenoid possessing an oxetane ring from *Mitrephora glabra*. *Org. Lett.* **7**, 5709–5712 (2005).
53. Groves, J. T., McClusky, G. A., White, R. E. & Coon, M. J. Aliphatic hydroxylation by highly purified liver microsomal cytochrome P-450. Evidence for a carbon radical intermediate. *Biochem. Biophys. Res. Commun.* **81**, 154–160 (1978).
54. Loskot, S. A., Romney, D. K., Arnold, F. H. & Stoltz, B. M. Enantioselective total synthesis of nigelladine A via late-stage C–H oxidation enabled by an engineered P450 enzyme. *J. Am. Chem. Soc.* **139**, 10196–10199 (2017).
55. Sheldon, R. A., Brady, D. & Bode, M. L. The hitchhiker's guide to biocatalysis: recent advances in the use of enzymes in organic synthesis. *Chem. Sci.* **11**, 2587–2605 (2020).
56. Winkler, C. K., Schrittwieser, J. H. & Kroutil, W. Power of biocatalysis for organic synthesis. *ACS Cent. Sci.* **7**, 55–71 (2021).
57. Arnold, F. H. Directed evolution: bringing new chemistry to life. *Angew. Chem. Int. Ed. Engl.* **57**, 4143–4148 (2018).
58. Wang, Y. et al. Directed evolution: methodologies and applications. *Chem. Rev.* **121**, 12384–12444 (2021).
59. Fasan, R. Tuning P450 enzymes as oxidation catalysts. *ACS Catal.* **2**, 647–666 (2012).
60. Rudolf, J. D., Dong, L.-B., Zhang, X., Renata, H. & Shen, B. Cytochrome P450-catalyzed hydroxylation initiating ether formation in platensimycin biosynthesis. *J. Am. Chem. Soc.* **140**, 12349–12353 (2018).
61. Dong, L.-B. et al. Cryptic and stereospecific hydroxylation, oxidation, and reduction in platensimycin and platencin biosynthesis. *J. Am. Chem. Soc.* **141**, 4043–4050 (2019).
62. Richter, M. J. R., Schneider, M., Brandstätter, M., Krautwald, S. & Carreira, E. M. Total synthesis of (−)-mitrephorone A. *J. Am. Chem. Soc.* **140**, 16704–16710 (2018).
63. Wein, L. A., Wurst, K., Angyal, P., Weisheit, L. & Magauer, T. Synthesis of (−)-mitrephorone A via a bioinspired late stage C–H oxidation of (−)-mitrephorone B. *J. Am. Chem. Soc.* **141**, 19589–19593 (2019).
64. Alekseychuk, M., Adrian, S., Heinze, R. C. & Heretsch, P. Biogenesis-inspired, divergent synthesis of spirochensilide A, spirochensilide B, and abifarine B employing a radical-polar crossover rearrangement strategy. *J. Am. Chem. Soc.* **144**, 11574–11579 (2022).
A synthesis using C–H oxidation to access carbocationic intermediates akin to those in the biosynthesis.
65. Long, X., Li, J., Gao, F., Wu, H. & Deng, J. Bioinspired synthesis of spirochensilide A from lanosterol. *J. Am. Chem. Soc.* **144**, 16292–16297 (2022).
A synthesis published contemporaneously with the above reference, using a similar oxidation.
66. Zhao, Q.-Q. et al. Spirochensilides A and B, two new rearranged triterpenoids from *Abies chensiensis*. *Org. Lett.* **17**, 2760–2763 (2015).
67. Wappes, E. A., Fosu, S. C., Chopko, T. C. & Nagib, D. A. Triiodide-mediated δ-amination of secondary C–H bonds. *Angew. Chem. Int. Ed. Engl.* **55**, 9974–9978 (2016).
68. Liang, X.-T., Chen, J.-H. & Yang, Z. Asymmetric total synthesis of (−)-spirochensilide A. *J. Am. Chem. Soc.* **142**, 8116–8121 (2020).
69. Yang, D., Wong, M.-K., Wang, X.-C. & Tang, Y.-C. Regioselective intramolecular oxidation of unactivated C–H bonds by dioxiranes generated in situ. *J. Am. Chem. Soc.* **120**, 6611–6612 (1998).
70. Wong, M.-K. et al. Investigation on the regioselectivities of intramolecular oxidation of unactivated C–H bonds by dioxiranes generated in situ. *J. Org. Chem.* **68**, 6321–6328 (2003).
71. Wong, M.-K., Chung, N.-W., He, L. & Yang, D. Substituent effects on regioselective intramolecular oxidation of unactivated C–H bonds: stereoselective synthesis of substituted tetrahydropyrans. *J. Am. Chem. Soc.* **125**, 158–162 (2003).
72. Kasuya, S., Kamijo, S. & Inoue, M. Direct construction of 1,3-diaxial diol derivatives by C–H hydroxylation. *Org. Lett.* **11**, 3630–3632 (2009).
73. Lane, J. F., Koch, W. T., Leeds, N. S. & Gorin, G. On the toxin of *Illicium anisatum*. I. The isolation and characterization of a convulsant principle: anisatin[1]. *J. Am. Chem. Soc.* **74**, 3211–3215 (1952).
74. Fukuyama, Y. & Huang, J.-M. in *Studies in Natural Products Chemistry* Vol. 32 (ed Atta-ur-Rahman) pp. 395–427 (Elsevier, 2005).
75. Concepción, J. I., Francisco, C. G., Hernández, R., Salazar, J. A. & Suárez, E. Intramolecular hydrogen abstraction. Iodosobenzene diacetate, an efficient and convenient reagent for alkoxy radical generation. *Tetrahedron Lett.* **25**, 1953–1956 (1984).
76. Chen, M. S. & White, M. C. A predictably selective aliphatic C–H oxidation reaction for complex molecule synthesis. *Science* **318**, 783–787 (2007).

77. Shen, Y. et al. Site-specific photochemical desaturation enables divergent syntheses of *Illicium* sesquiterpenes. *J. Am. Chem. Soc.* **143**, 3256–3263 (2021).
A synthesis that uses a versatile late-stage desaturation as a means of installing several different functional groups.
78. Condakes, M. L., Hung, K., Harwood, S. J. & Maimone, T. J. Total syntheses of (−)-majucin and (−)-jiadifenoxolane A, complex majucin-type *Illicium* sesquiterpenes. *J. Am. Chem. Soc.* **139**, 17783–17786 (2017).
79. Condakes, M. L., Novaes, L. F. T. & Maimone, T. J. Contemporary synthetic strategies toward seco-prezizaane sesquiterpenes from *Illicium* species. *J. Org. Chem.* **83**, 14843–14852 (2018).
80. Marco-Martínez, J., López-Carrillo, V., Buñuel, E., Simancas, R. & Cárdenas, D. J. Pd-catalyzed borylative cyclization of 1,6-enynes. *J. Am. Chem. Soc.* **129**, 1874–1875 (2007).
81. Camelio, A. M., Barton, T., Guo, F., Shaw, T. & Siegel, D. Hydroxyl-directed cyclizations of 1,6-enynes. *Org. Lett.* **13**, 1517–1519 (2011).
82. Berkessel, A., Adrio, J. A., Hüttenhain, D. & Neudörfl, J. M. Unveiling the "booster effect" of fluorinated alcohol solvents: aggregation-induced conformational changes and cooperatively enhanced H-bonding. *J. Am. Chem. Soc.* **128**, 8421–8426 (2006).
83. Huang, J., Yokoyama, R., Yang, C. & Fukuyama, Y. Merrilactone A, a novel neurotrophic sesquiterpene dilactone from *Illicium merrillianum*. *Tetrahedron Lett.* **41**, 6111–6114 (2000).
84. Kouno, I., Mori, K., Okamoto, S. & Sato, S. Structures of anislactone A and B; novel type of sesquiterpene lactones from the pericarps of *Illicium anisatum*. *Chem. Pharm. Bull.* **38**, 3060–3063 (1990).
85. Inoue, M., Sato, T. & Hirama, M. Asymmetric total synthesis of (−)-merrilactone A: use of a bulky protecting group as long-range stereocontrolling element. *Angew. Chem. Int. Ed. Engl.* **45**, 4843–4848 (2006).
86. Chen, J. et al. Total synthesis of (±)-merrilactone A. *Angew. Chem. Int. Ed. Engl.* **51**, 5897–5899 (2012).
87. Crossley, S. W. M., Tong, G., Lambrecht, M. J., Burdge, H. E. & Shenvi, R. A. Synthesis of (−)-picrotoxinin by late-stage strong bond activation. *J. Am. Chem. Soc.* **142**, 11376–11381 (2020).
A synthesis that uses C–H oxidation not only to construct the heterocyclic core but also to excise an unwanted methyl group.
88. Porter, L. A. Picrotoxinin and related substances. *Chem. Rev.* **67**, 441–464 (1967).
89. Corey, E. J. & Pearce, H. L. Total synthesis of picrotoxinin. *J. Am. Chem. Soc.* **101**, 5841–5843 (1979).
90. Corey, E. J. & Pearce, H. L. Total synthesis of picrotin. *Tetrahedron Lett.* **21**, 1823–1824 (1980).
91. Niwa, H. et al. Stereocontrolled total synthesis (−)-picrotoxinin and (+)-coriamyrtin via a common isotwistane intermediate. *J. Am. Chem. Soc.* **106**, 4547–4552 (1984).
92. Miyashita, M., Suzuki, T. & Yoshikoshi, A. Stereoselective total synthesis of (−)-picrotoxinin and (−)-picrotin. *J. Am. Chem. Soc.* **111**, 3728–3734 (1989).
93. Trost, B. M. & Krische, M. J. General strategy for the asymmetric synthesis of the picrotoxanes. *J. Am. Chem. Soc.* **118**, 233–234 (1996).
94. Trost, B. & Krische, M. J. Palladium-catalyzed enyne cycloisomerization reaction in an asymmetric approach to the picrotoxane sesquiterpenes. 2. Second-generation total syntheses of corianin, picrotoxinin, picrotin, and methyl picrotoxate. *J. Am. Chem. Soc.* **121**, 6131–6141 (1999).
95. Trost, B. M., Haffner, C. D., Jebaratnam, D. J., Krische, M. J. & Thomas, A. P. The palladium-catalyzed enyne cycloisomerization reaction in a general approach to the asymmetric syntheses of the picrotoxane sesquiterpenes. Part I. First-generation total synthesis of corianin and formal syntheses of picrotoxinin and picrotin. *J. Am. Chem. Soc.* **121**, 6183–6192 (1999).
96. Cao, J. et al. Synthesis of the tricyclic picrotoxane motif by an oxidative cascade cyclization. *Org. Lett.* **21**, 4896–4899 (2019).
97. Hong, B., Luo, T. & Lei, X. Late-stage diversification of natural products. *ACS Cent. Sci.* **6**, 622–635 (2020).
98. Kim, K. E., Kim, A. N., McCormick, C. J. & Stoltz, B. M. Late-stage diversification: a motivating force in organic synthesis. *J. Am. Chem. Soc.* **143**, 16890–16901 (2021).
99. Oeschger, R. et al. Diverse functionalization of strong alkyl C–H bonds by undirected borylation. *Science* **368**, 736–741 (2020).
100. Carestia, A. M., Ravelli, D. & Alexanian, E. J. Reagent-dictated site selectivity in intermolecular aliphatic C–H functionalizations using nitrogen-centered radicals. *Chem. Sci.* **9**, 5360–5365 (2018).
101. Wang, J. et al. A biocatalytic hydroxylation-enabled unified approach to C19-hydroxylated steroids. *Nat. Commun.* **10**, 3378 (2019).
102. Fraga, B. M. The trachylobane diterpenes. *Phytochem. Anal.* **5**, 49–56 (1994).
A synthesis that takes advantage of the electron-releasing cyclopropane-containing skeleton of the natural product to enable site-selective C–H oxidation.
103. Wein, L. A., Wurst, K. & Magauer, T. Total synthesis and late-stage C–H oxidations of *ent*-trachylobane natural products. *Angew. Chem. Int. Ed. Engl.* **61**, e202113829 (2022).
104. Bovicelli, P., Lupattelli, P., Mincione, E., Prencipe, T. & Curci, R. Oxidation of natural targets by dioxiranes. 2. Direct hydroxylation at the side chain C-25 of cholestane derivatives and of vitamin D_3 Windaus–Grundmann ketone. *J. Org. Chem.* **57**, 5052–5054 (1992).
105. Zou, L. et al. Enhanced reactivity in dioxirane C–H oxidations via strain release: a computational and experimental study. *J. Org. Chem.* **78**, 4037–4048 (2013).
106. Kawamata, Y. et al. Scalable, electrochemical oxidation of unactivated C–H bonds. *J. Am. Chem. Soc.* **139**, 7448–7451 (2017).
107. Wang, C., Shalyaev, K. V., Bonchio, M., Carofiglio, T. & Groves, J. T. Fast catalytic hydroxylation of hydrocarbons with ruthenium porphyrins. *Inorg. Chem.* **45**, 4769–4782 (2006).
108. Vicens, L., Bietti, M. & Costas, M. General access to modified α-amino acids by bioinspired stereoselective γ-C–H bond lactonization. *Angew. Chem. Int. Ed. Engl.* **60**, 4740–4746 (2021).
A synthesis featuring a late-stage highly efficient, triply-operative aromatic C–H oxidation.
109. Zhao, P., Guo, Y. & Luan, X. Total synthesis of dalesconol A by Pd(0)/norbornene-catalyzed three-fold domino reaction and Pd(II)-catalyzed trihydroxylation. *J. Am. Chem. Soc.* **143**, 21270–21274 (2021).
110. Zhang, Y. L. et al. Unprecedented immunosuppressive polyketides from *Daldinia eschscholzii*, a mantis-associated fungus. *Angew. Chem. Int. Ed. Engl.* **47**, 5823–5826 (2008).
111. Neufeldt, S. R. & Sanford, M. S. *O*-Acetyl oximes as transformable directing groups for Pd-catalyzed C–H bond functionalization. *Org. Lett.* **12**, 532–535 (2010).
112. Horwitz, M. A. Local desymmetrization as an engine of stereochemical elaboration in total synthesis. *Tetrahedron Lett.* **97**, 153776 (2022).
113. Bai, L. et al. Palladium/norbornene-catalyzed C–H alkylation/alkyne insertion/indole dearomatization domino reaction: assembly of spiroindolenine-containing pentacyclic frameworks. *Angew. Chem. Int. Ed. Engl.* **57**, 5151–5155 (2018).
114. Nan, J., Yuan, Y., Bai, L., Liu, J. & Luan, X. Highly chemoselective construction of spiro[4,5] decane-embedded polycyclic scaffolds by a palladium/norbornene-catalyzed C–H activation/arene dearomatization reaction. *Org. Lett.* **20**, 7731–7734 (2018).
115. Mo, F., Trzepkowski, L. J. & Dong, G. Synthesis of ortho-acylphenols through the palladium-catalyzed ketone-directed hydroxylation of arenes. *Angew. Chem. Int. Ed. Engl.* **51**, 13075–13079 (2012).
116. Liang, Y.-F. et al. Ligand-promoted Pd-catalyzed oxime ether directed C–H hydroxylation of arenes. *ACS Catal.* **5**, 6148–6152 (2015).
117. Diao, T. & Stahl, S. S. Synthesis of cyclic enones via direct palladium-catalyzed aerobic dehydrogenation of ketones. *J. Am. Chem. Soc.* **133**, 14566–14569 (2011).
118. Kim, J. & Chang, S. Iridium-catalyzed direct CH amidation with weakly coordinating carbonyl directing groups under mild conditions. *Angew. Chem. Int. Ed. Engl.* **53**, 2203–2207 (2014).
119. Ashley, J. N., Hobbs, B. C. & Raistrick, H. Studies in the biochemistry of micro-organisms: the crystalline colouring matters of *Fusarium culmorum* (W. G. Smith) Sacc. and related forms. *Biochem. J.* **31**, 385–397 (1937).
120. Briggs, L. H. & Sutherland, M. D. The essential oil of *Cupressus macrocarpa*. *J. Org. Chem.* **07**, 397–407 (1942).
121. Akiyoshi, S., Erdtman, H. & Kubota, T. Chemistry of the natural order cupressales — XXVI: the identity of junipene, kuromatsuene and longifolene and of juniperol, kuromatsuol, macrocarpol and longiborneol. *Tetrahedron* **9**, 237–239 (1960).
122. Barton, D. H. R. & Werstiuk, N. H. Sesquiterpenoids. Part XIV. The constitution and stereochemistry of culmorin. *J. Chem. Soc. C Org.* https://doi.org/10.1039/J39680000148 (1968).
123. Kasitu, G. C. et al. Isolation and characterization of culmorin derivatives produced by *Fusarium culmorum* CMI 14764. *Can. J. Chem.* **70**, 1308–1316 (1992).
124. Alam, M., Jones, E. B. G., Hossain, M. B. & van der Helm, D. Isolation and structure of isoculmorin from the marine fungus *Kallichroma tethys*. *J. Nat. Prod.* **59**, 454–456 (1996).
125. Bahadoor, A. et al. Hydroxylation of longiborneol by a *Clm2*-encoded CYP450 monooxygenase to produce culmorin in *Fusarium graminearum*. *J. Nat. Prod.* **79**, 81–88 (2016).
126. Masarwa, A., Weber, M. & Sarpong, R. Selective C–C and C–H bond activation/cleavage of pinene derivatives: synthesis of enantiopure cyclohexenone scaffolds and mechanistic insights. *J. Am. Chem. Soc.* **137**, 6327–6334 (2015).
127. Lusi, R. F., Perea, M. A. & Sarpong, R. C–C bond cleavage of α-pinene derivatives prepared from carvone as a general strategy for complex molecule synthesis. *Acc. Chem. Res.* **55**, 746–758 (2022).
128. Chen, M. S. & White, M. C. Combined effects on selectivity in Fe-catalyzed methylene oxidation. *Science* **327**, 566–571 (2010).
Codifies selectivity rules in undirected C–H oxidation using iron oxo complexes.
129. Simmons, E. M. & Hartwig, J. F. Catalytic functionalization of unactivated primary C–H bonds directed by an alcohol. *Nature* **483**, 70–73 (2012).
130. Li, B., Driess, M. & Hartwig, J. F. Iridium-catalyzed regioselective silylation of secondary alkyl C–H bonds for the synthesis of 1,3-diols. *J. Am. Chem. Soc.* **136**, 6586–6589 (2014).
131. Ma, X., Kucera, R., Goethe, O. F., Murphy, S. K. & Herzon, S. B. Directed C–H bond oxidation of (+)-pleuromutilin. *J. Org. Chem.* **83**, 6843–6892 (2018).
132. Karmel, C., Li, B. & Hartwig, J. F. Rhodium-catalyzed regioselective silylation of alkyl C–H bonds for the synthesis of 1,4-diols. *J. Am. Chem. Soc.* **140**, 1460–1470 (2018).
133. Nakazaki, M. & Naemura, K. Photolyses of isobornyl and bornyl nitrites. *Bull. Chem. Soc. Jpn.* **37**, 532–535 (1964).
134. Renata, H., Zhou, Q. & Baran, P. S. Strategic redox relay enables a scalable synthesis of ouabagenin, a bioactive cardenolide. *Science* **339**, 59–63 (2013).
135. Berger, M., Knittl-Frank, C., Bauer, S., Winter, G. & Maulide, N. Application of relay C–H oxidation logic to polyhydroxylated oleanane triterpenoids. *Chem* **6**, 1183–1189 (2020).
136. Desai, L. V., Hull, K. L. & Sanford, M. S. Palladium-catalyzed oxygenation of unactivated sp^3 C–H bonds. *J. Am. Chem. Soc.* **126**, 9542–9543 (2004).
137. Trotta, A. H. Total synthesis of oridamycins A and B. *Org. Lett.* **17**, 3358–3361 (2015).

138. Trotta, A. H. Toward a unified total synthesis of the xiamycin and oridamycin families of indolosesquiterpenes. *J. Org. Chem.* **82**, 13500–13516 (2017).
139. Corey, E. J., Niimura, K., Konishi, Y., Hashimoto, S. & Hamada, Y. A new synthetic route to prostaglandins. *Tetrahedron Lett.* **27**, 2199–2202 (1986).
140. Siler, D. A., Mighion, J. D. & Sorensen, E. J. An enantiospecific synthesis of jiadifenolide. *Angew. Chem. Int. Ed. Engl.* **53**, 5332–5335 (2014).
141. Fan, Y.-Y. et al. Cephanolides A–J, cephalotane-type diterpenoids from cephalotaxus sinensis. *J. Nat. Prod.* **80**, 3159–3166 (2017).
142. Ge, Z.-P. et al. Cephalotane-type norditerpenoids from *Cephalotaxus fortunei* var. *alpina*. *Chin. J. Chem.* **40**, 1177–1184 (2022).
143. Xu, L., Wang, C., Gao, Z. & Zhao, Y.-M. Total synthesis of (±)-cephanolides B and C via a palladium-catalyzed cascade cyclization and late-stage sp^3 C–H bond oxidation. *J. Am. Chem. Soc.* **140**, 5653–5658 (2018).
144. Zhang, H., He, H. & Gao, S. Asymmetric total synthesis of cephanolide A. *Angew. Chem. Int. Ed. Engl.* **59**, 20417–20422 (2020).
145. Zhang, H., He, H. & Gao, S. Asymmetric total synthesis of cephanolide B. *Org. Chem. Front.* **8**, 555–559 (2021).
146. Lu, Y., Xu, M.-M., Zhang, Z.-M., Zhang, J. & Cai, Q. Catalytic asymmetric inverse-electron-demand Diels–Alder reactions of 2-pyrones with indenes: total syntheses of cephanolides A and B. *Angew. Chem. Int. Ed. Engl.* **60**, 26610–26615 (2021).
147. Li, A., He, Z., Liu, B., Yang, Z. & Zhang, Z. Stereoselective synthesis of (±)-cephanolide B. *Org. Lett.* **23**, 9237–9240 (2021).
148. Qing, Z., Mao, P., Wang, T. & Zhai, H. Asymmetric total syntheses of cephalotane-type diterpenoids cephanolides A–D. *J. Am. Chem. Soc.* **144**, 10640–10646 (2022).
149. Sun, Z. et al. Total synthesis of (−)-ceforalide B and (−)-cephanolides B–D. *Org. Lett.* **24**, 7507–7511 (2022).
150. Marth, C. J. et al. Network-analysis-guided synthesis of weisaconitine D and liljestrandinine. *Nature* **528**, 493–498 (2015).
151. Doering, N. A., Sarpong, R. & Hoffmann, R. W. A case for bond-network analysis in the synthesis of bridged polycyclic complex molecules: hetidine and hetisine diterpenoid alkaloids. *Angew. Chem. Int. Ed. Engl.* **59**, 10722–10731 (2020).
152. Corey, E. J., Howe, W. J., Orf, H. W., Pensak, D. A. & Petersson, G. General methods of synthetic analysis. Strategic bond disconnections for bridged polycyclic structures. *J. Am. Chem. Soc.* **97**, 6116–6124 (1975).
153. Molander, G. A. & Sandrock, D. L. Utilization of potassium vinyltrifluoroborate in the development of a 1,2-dianion equivalent. *Org. Lett.* **11**, 2369–2372 (2009).
154. Su, W. et al. Ligand-controlled regiodivergent copper-catalyzed alkylboration of alkenes. *Angew. Chem. Int. Ed. Engl.* **54**, 12957–12961 (2015).
155. Liu, Z., Gao, Y., Zeng, T. & Engle, K. M. Transition-metal-catalyzed 1,2-carboboration of alkenes: strategies, mechanisms, and stereocontrol. *Isr. J. Chem.* **60**, 219–229 (2020).
156. Clausen, F., Kischkewitz, M., Bergander, K. & Studer, A. Catalytic protodeboronation of pinacol boronic esters: formal anti-Markovnikov hydromethylation of alkenes. *Chem. Sci.* **10**, 6210–6214 (2019).
157. Miyai, T., Ueba, M. & Baba, A. Novel synthetic usage of indium compounds as catalyst: reductive deoxygenation of aryl ketones and *sec*-benzylic alcohols. *Synlett* **1999**, 182–184 (1999).
158. Yasuda, M., Onishi, Y., Ueba, M., Miyai, T. & Baba, A. Direct reduction of alcohols: highly chemoselective reducing system for secondary or tertiary alcohols using chlorodiphenylsilane with a catalytic amount of indium trichloride. *J. Org. Chem.* **66**, 7741–7744 (2001).
159. Yuan, C. et al. Metal-free oxidation of aromatic carbon–hydrogen bonds through a reverse-rebound mechanism. *Nature* **499**, 192–196 (2013).
160. Berger, F. et al. Site-selective and versatile aromatic C–H functionalization by thianthrenation. *Nature* **567**, 223–228 (2019).
161. Li, Z.-Y. & Wang, G.-W. Palladium-catalyzed decarboxylative *ortho*-ethoxycarbonylation of *O*-methyl ketoximes and 2-arylpyridines with potassium oxalate monoester. *Org. Lett.* **17**, 4866–4869 (2015).
162. Weitz, D. J. & Bednarski, M. D. Synthesis of acyclic sugar aldehydes by ozonolysis of oximes. *J. Org. Chem.* **54**, 4957–4959 (1989).
163. Li, G.-X. et al. A unified photoredox-catalysis strategy for $C(sp^3)$–H hydroxylation and amidation using hypervalent iodine. *Chem. Sci.* **8**, 7180–7185 (2017).

Author contributions

I.B. contributed to the discussion of content, researching, and writing and editing of this manuscript. R.F.L. helped in the manuscript conception, contributed to the discussion of content, researching, writing the case study and editing of the manuscript. S.W. contributed to the discussion of content, researching, writing the case study and editing of the manuscript. J.H.C. contributed to the discussion of content and editing of the manuscript. R.S. contributed to the conception and direction of the manuscript, discussion of content and editing of the manuscript.

Competing interests

The authors declare no competing interests.

Additional information

Peer review information *Nature Reviews Chemistry* thanks the anonymous reviewers for their contribution to the peer review of this work.

Publisher's note Springer Nature remains neutral with regard to jurisdictional claims in published maps and institutional affiliations.